Automated Symbolic Upscaling: Model Generation for Extended Applicability Regimes, Part 2

Kyle Pietrzyk[1], **Ilenia Battiato**[1]

[1]Department of Energy Resources Engineering, Stanford University, 367 Panama St., Stanford, CA 94305

Key Points:

- An algorithmic procedure for applying the homogenization strategy from Part 1 is encoded into Symbolica, an automated upscaling framework.
- Using the strategy, Symbolica automatically defines valid closure forms and closure problems for two reactive mass transport problems.
- Nontrivial homogenized models for complex problems are produced by Symbolica and numerically validated.

Corresponding author: Ilenia Battiato, ibattiat@stanford.edu

Abstract

In this second part of the two paper series, we detail an algorithmic procedure for systematically implementing the generalized closure form strategy presented in Part 1. After encoding the algorithm into Symbolica, an automated upscaling framework, we upscale two reactive mass transport problems and numerically validate the resulting nonlinear homogenized models. In both problems, nontrivial closure forms and closure problems are automatically formulated using the encoded strategy with no human interaction, nor prior knowledge regarding the closure required for the systems. We hope these demonstrations spark further interest in automated analytical frameworks for multi-scale modeling, as such capabilities are invaluable for generating rigorous multiscale models of complex phenomena in geological porous media.

1 Introduction

In Part 1 of this series, we presented a general analytical upscaling strategy for extending model applicability with respect to classical homogenization theory. This strategy involved generalizing the assumed form of ordered solutions to enable valid closure problem formulation. In short, assumed solution forms were constructed as linear combinations of closure terms, which were chosen based on the equations for which closure was sought. The implementation of this strategy was detailed in two reactive mass transport systems: the first considered a single solute undergoing a linear heterogeneous reaction, and the second considered two solutes undergoing linear heterogeneous reactions. Homogenized models were derived for both systems in moderately reactive regimes, where classical homogenization theory fails due to similar magnitudes of diffusive and reactive terms. Nontrivial terms and effective parameters that coupled reactive, diffusive, and advective physics were found and discussed in detail. Then, numerical validation of the models was provided to justify the proposed upscaling strategy. In light of the results, we found agreement with previous works (Auriault & Adler, 1995; Battiato & Tartakovsky, 2011; Boso & Battiato, 2013; Bloch & Auriault, 2019; Iliev et al., 2020) advising caution against assuming the forms of macroscopic equations from the forms of their microscopic counterparts, as they may vastly differ depending on the physical regime due to nontrivial couplings and emergent terms.

Now, in Part 2, we detail an algorithmic procedure for generally applying our strategy and encode it into Symbolica, our automated upscaling framework (Pietrzyk et al., 2021). Symbolica generates upscaled models for multi-physical systems involving porous media by automating rigorous upscaling procedures using symbolic computation. Using our encoded algorithm, we employ Symbolica to homogenize two reactive mass transport systems: the first considers a single solute undergoing a nonlinear heterogeneous reaction, and the second considers a multi-component system undergoing linear and nonlinear, homogeneous and heterogeneous reactions. We emphasize that the encoded strategy enables Symbolica to automatically define appropriate closure forms and valid closure problems for these systems without human interaction. Considering moderately reactive regimes, nonlinear homogenized models with concentration-dependent effective parameters and emergent terms are derived. Upon numerically validating the models, we verify our encoded strategy and demonstrate the high implementation efficiency of the generalized closure form strategy, as its encoding generalizes to a broad range of multi-physical systems involving geological porous media.

The manuscript is organized as follows. In Section 2, an algorithmic procedure is detailed for the systematic execution of the generalized closure form strategy presented in Part 1. After encoding Symbolica with this procedure, we use the automated strategy to homogenize a single-species system undergoing a nonlinear heterogeneous reaction in Section 3, where the homogenized results and numerical validation are provided in Subsections 3.1 and 3.2, respectively. We then homogenize a multi-species system undergoing multiple linear and nonlinear, homogeneous and heterogeneous reactions in Section 4, where the homogenized results and numerical validation are provided in Subsections 4.1 and 4.2, respectively. Finally, a summary of Part 2 is presented in Section 5.

2 The Generalized Closure Form Strategy Procedure

Here, we introduce an algorithmic procedure for broadly implementing the generalized closure form strategy outlined in Part 1 of this series. This procedure will serve as a roadmap for encoding the strategy into automated upscaling frameworks like Symbolica. While further details regarding Symbolica and its homogenization procedure can be found in our previous work (Pietrzyk et al., 2021), we focus on describing the procedure for executing the strategy in a systematic fashion.

1.) Identify the inhomogeneous terms of the system

$$\mathscr{F}[c_1] = -\mathbf{A}(\boldsymbol{\xi}) \cdot \mathbf{F}(t,\mathbf{x}) - \mathbf{B} \cdot \mathbf{F}(t,\mathbf{x}) + \frac{|\Gamma|}{|\mathcal{B}|} a(t,\mathbf{x}) + \nabla_{\boldsymbol{\xi}} \cdot \mathbf{F}(t,\mathbf{x}) \quad \text{in } \mathcal{B}$$

$$\mathscr{G}[c_1] = -\mathbf{n} \cdot \mathbf{F}(t,\mathbf{x}) + a(t,\mathbf{x}) \quad \text{on } \Gamma$$

2.) Use linearity to create a partial-solution and subsystem for each inhomogeneous term

$$c_1 = c_1^{\{1\}} + c_1^{\{2\}} + c_1^{\{3\}} + c_1^{\{4\}} + c_1^{\{5\}} + c_1^{\{6\}}$$

$$\mathscr{F}\left[c_1^{\{1\}}\right] = -\mathbf{A}(\boldsymbol{\xi}) \cdot \mathbf{F}(t,\mathbf{x}) \qquad \mathscr{G}\left[c_1^{\{1\}}\right] = 0$$

$$\mathscr{F}\left[c_1^{\{2\}}\right] = -\mathbf{B} \cdot \mathbf{F}(t,\mathbf{x}) \qquad \mathscr{G}\left[c_1^{\{2\}}\right] = 0$$

$$\mathscr{F}\left[c_1^{\{3\}}\right] = \frac{|\Gamma|}{|\mathcal{B}|} a(t,\mathbf{x}) \qquad \mathscr{G}\left[c_1^{\{3\}}\right] = 0$$

$$\vdots \qquad\qquad \vdots$$

3.) Consider valid closure forms for each partial-solution

$$c_1^{\{1\}} \in \left\{ \boldsymbol{\chi}_1^{\{1\}} \cdot \mathbf{F}(t,\mathbf{x}) + \overline{c}_1^{\{1\}} \right\}$$

$$c_1^{\{2\}} \in \left\{ \chi_1^{\{2\}} [\mathbf{B} \cdot \mathbf{F}(t,\mathbf{x})] + \overline{c}_1^{\{2\}}, \; \boldsymbol{\chi}_1^{\{2\}} \cdot \mathbf{F}(t,\mathbf{x}) + \overline{c}_1^{\{2\}} \right\}$$

$$c_1^{\{3\}} \in \left\{ \chi_1^{\{3\}} a(t,\mathbf{x}) + \overline{c}_1^{\{3\}} \right\}$$

$$\vdots$$

4.) Combine subsystems that emit partial-solutions of similar forms

Combine subsystems for $c_1^{\{1\}}$, $c_1^{\{2\}}$, $c_1^{\{4\}}$, $c_1^{\{5\}}$:

$$\mathscr{F}\left[c_1^{[1]}\right] = -\mathbf{A}(\boldsymbol{\xi}) \cdot \mathbf{F}(t,\mathbf{x}) - \mathbf{B} \cdot \mathbf{F}(t,\mathbf{x}) + \nabla_{\boldsymbol{\xi}} \cdot \mathbf{F}(t,\mathbf{x})$$

$$\mathscr{G}\left[c_1^{[1]}\right] = -\mathbf{n} \cdot \mathbf{F}(t,\mathbf{x})$$

$$c_1^{[1]} = \boldsymbol{\chi}_1^{[1]} \cdot \mathbf{F}(t,\mathbf{x}) + \overline{c}_1^{[1]}$$

Combine subsystems for $c_1^{\{3\}}$, $c_1^{\{6\}}$:

$$\mathscr{F}\left[c_1^{[2]}\right] = \frac{|\Gamma|}{|\mathcal{B}|} a(t,\mathbf{x})$$

$$\mathscr{G}\left[c_1^{[2]}\right] = a(t,\mathbf{x})$$

$$c_1^{[2]} = \chi_1^{[2]} a(t,\mathbf{x}) + \overline{c}_1^{[2]}$$

where $c_1 = c_1^{[1]} + c_1^{[2]}$

5.) Substitute partial-solutions into newly formed subsystems and simplify to obtain closure problems

Closure Problem 1:

$$\mathscr{F}\left[\boldsymbol{\chi}_1^{[1]}\right] = -\mathbf{A}(\boldsymbol{\xi}) - \mathbf{B} + \nabla_{\boldsymbol{\xi}} \cdot \mathbf{I} \quad \text{in } \mathcal{B}$$

$$\mathscr{G}\left[\boldsymbol{\chi}_1^{[1]}\right] = -\mathbf{n} \cdot \mathbf{I} \quad \text{on } \Gamma$$

Closure Problem 2:

$$\mathscr{F}\left[\chi_1^{[2]}\right] = \frac{|\Gamma|}{|\mathcal{B}|} \quad \text{in } \mathcal{B}$$

$$\mathscr{G}\left[\chi_1^{[2]}\right] = 1 \quad \text{on } \Gamma$$

Figure 1. The step-by-step, algorithmic procedure Symbolica executes to implement the generalized closure form strategy for automatic closure form and closure problem formulation. The example problem considered generalizes the first order system from the first problem of Part 1 (equations (A8*) and (A6b*)).

In Figure 1, the generalized closure form strategy is implemented on an example problem in a step-by-step, algorithmic procedure. The problem considered is a generalization of the first order system from the first problem of Part 1 (equations (A8*) and (A6b*))[1]. Here, $\mathbf{A}(\boldsymbol{\xi})$ is a general vector that depends on $\boldsymbol{\xi}$, $\mathbf{F}(t,\mathbf{x})$ is a general vector that depends on t and $\mathbf{x}$, $\mathbf{B}$ is a general vector with no dependencies, $a(t,\mathbf{x})$ is a general scalar that depends on t and $\mathbf{x}$, and $\mathbf{n}$ is the normal vector to the interface Γ. For simplicity, we assume $\mathscr{F}[\cdot]$ and $\mathscr{G}[\cdot]$ are linear, homogeneous differential operators that only operate with fast variables and allow for the separation of fast and slow variables (e.g., the operators from the first order system in the first problem of Part 1). However, the algorithmic procedure can be generalized to other operators and systems involving multiple equations and boundary conditions through various extensions. Similarly, the procedure generalizes to more complex inhomogeneous terms than those shown in Step 1 of Figure 1 (e.g., inhomogeneous terms involving tensor products, double-dot products, cross products, etc.).

To begin the procedure, inhomogeneous terms in the equations and boundary conditions are identified. As shown in Step 1 of Figure 1, the N_{IH} $(= 6)$ inhomogeneous terms in the system are differentiated by color. Then, the solution c_1 is represented as the sum of *partial-solutions* $c_1^{\{k\}}$, where $k \in \{m \in \mathbb{Z}^+ : m \leq N_{\text{IH}}\}$, and the linearity of the system is used to create subsystems such that each partial-solution accommodates a single inhomogeneous term (Step 2). With the system partitioned in this manner, valid closure forms are generated for each partial-solution based on the paired inhomogeneous term (Step 3). While various methods can be used to generate the forms, *valid* closure forms allow for sub-

[1] Equation, system, table, and figure numbers followed by the superscript "*" refer to entities from Part 1.

systems to become independent of the slow variables (i.e., t and $\mathbf{x}$) upon substitution and simplification. We note that multiple valid closure forms may exist for a single partial-solution (e.g., $c_1^{\{2\}}$ in Step 3). While only one valid closure form is required for each partial-solution, identifying multiple valid forms is advantageous in the remaining steps of the procedure. In Step 4, subsystems that emit partial-solutions of similar forms are added together to reduce the total number of subsystems (e.g., the subsystems corresponding to $c_1^{\{1\}}$, $c_1^{\{2\}}$, $c_1^{\{4\}}$, and $c_1^{\{5\}}$ are added together to create a new subsystem whose solution is $c_1^{[1]}$). Since the closure problems of the homogenized model are derived from the subsystems in Step 5, minimizing the number of subsystems ultimately reduces the overall computational expense of the homogenized model. We note that multiple ways in which subsystems can be added together may exist, and therefore, Step 4 offers an opportunity to develop methods for combining subsystems and obtaining the least number of closure problems. In Symbolica, subsystems are added together beginning with those that emit partial-solutions containing closure variables of the highest tensor order. Finally, in Step 5, the partial-solution forms are substituted into their respective subsystem and simplified to obtain valid closure problems.

As demonstrated in Part 1, formulating homogenized models in moderately reactive regimes may require nontrivial closure forms to be assumed and multiple closure problems to be defined. This further complicates the already intractable procedures necessary for homogenizing complex geological systems with the task of assuming valid solution forms for partial differential equations, which is traditionally handled by analytical "trial-and-error". Yet, in combination with Symbolica, our proposed algorithm surpasses this obstacle and enables fully automated symbolic homogenization in moderately reactive regimes. Without any human interaction, our algorithmic procedure enables Symbolica to (i) define valid closure forms based on the inhomogeneous terms in an equation and (ii) formulate a reduced number of valid closure problems for homogenization. Beyond the analysis of subsurface engineering applications with realistic complexities, this ability is invaluable for advancing automated symbolic computational methods as a whole, as problem solving techniques that utilize assumed solution forms are ubiquitous in applied mathematics.

3 Nonlinear Heterogeneous Reaction: One Species

We now homogenize the mass transport of a single species undergoing a nonlinear heterogeneous reaction using our algorithm encoded in Symbolica and verify the result. The equations governing the reactive transport are written as

$$\frac{\partial \hat{c}_\epsilon}{\partial \hat{t}} + \hat{\nabla} \cdot \left(\hat{\mathbf{u}}_\epsilon \hat{c}_\epsilon - \hat{D} \hat{\nabla} \hat{c}_\epsilon \right) = 0 \quad \text{in } \hat{\mathcal{B}}_\epsilon, \tag{1a}$$

subject to

$$-\mathbf{n} \cdot \hat{D} \hat{\nabla} \hat{c}_\epsilon = \hat{\mathcal{K}} \left(\hat{c}_\epsilon^2 - \hat{C}^2 \right) \quad \text{on } \hat{\Gamma}_\epsilon. \tag{1b}$$

With respect to the notation defined in Part 1, system (1) can be obtained from system (4*) by letting $N = 1$, $N_\Gamma = 1$, $i \in \{1\}$, $j \in \{1\}$, $\hat{R}_\epsilon^{(i)} = 0$, $p_{SNL}^{(i,j,k,l)} = 0$, and $\hat{\mathcal{K}}_{SL}^{(i,j,k)} = 0$, and simplifying the notation of the remaining variables to $\{\hat{c}_\epsilon^{(1)}, \hat{\mathcal{C}}^{(1)}, \hat{D}^{(1)}, \hat{\Gamma}_\epsilon^{(1)}, \mathbf{n}^{(1)}, \hat{\mathcal{K}}_{SNL}^{(1,1,1,1)}, \hat{C}_{SNL}^{(1,1,1,1)}\} = \{\hat{c}_\epsilon, \hat{\mathcal{C}}, \hat{D}, \hat{\Gamma}_\epsilon, \mathbf{n}, \hat{\mathcal{K}}, \hat{C}\}$. To scale the system, Symbolica uses the relevant nondimensionalizations from equation (5*) to obtain

$$\frac{\partial c_\epsilon}{\partial t} + \nabla \cdot (\mathrm{Pe} \mathbf{u}_\epsilon c_\epsilon - D \nabla c_\epsilon) = 0 \quad \text{in } \mathcal{B}_\epsilon, \tag{2a}$$

subject to

$$-\mathbf{n} \cdot D \nabla c_\epsilon = \mathrm{Da} \left(c_\epsilon^2 - \theta \right) \quad \text{on } \Gamma_\epsilon, \tag{2b}$$

where the Péclet number Pe, Damköhler number Da, and concentration ratio θ are defined as

$$\mathrm{Pe} = \frac{\hat{\mathcal{U}} \hat{\mathcal{L}}}{\hat{\mathcal{D}}}, \quad \mathrm{Da} = \frac{\hat{\mathcal{K}} \hat{\mathcal{L}} \hat{\mathcal{C}}}{\hat{\mathcal{D}}}, \quad \theta = \frac{\hat{C}^2}{\hat{\mathcal{C}}^2}. \tag{3}$$

In addition to the previous syntactic simplifications, we note that $\mathrm{Da} = \mathrm{Da}_{SNL}^{(1,1,1,1)}$ and $\theta = \theta_{SNL}^{(1,1,1,1)}$ with respect to the notation used in system (7*) and equation (8*).

We homogenize the system for a moderately reactive scenario, where diffusive and reactive terms are of similar order, i.e.,

$$\mathrm{Pe} \sim \mathcal{O}(\epsilon^{-1}), \quad \mathrm{Da} \sim \mathcal{O}(\epsilon^{0}), \quad \theta \sim \mathcal{O}(\epsilon^{0}). \tag{4}$$

In doing so, we trigger our encoded algorithm in Symbolica and are able to verify its implementation.

3.1 Homogenized Results

The total execution time for Symbolica to homogenize system (2) for $\langle c \rangle_Y = \langle c_0 \rangle_Y + \epsilon \langle c_1 \rangle_Y + \mathcal{O}(\epsilon^2)$ with $\mathcal{O}(\epsilon)$ error is 18 seconds. The closure form Symbolica generated for homogenization is written as

$$c_1 = \boldsymbol{\chi}^{[1]} \cdot \nabla_{\mathbf{x}} c_0 + \left(c_0^2 - \theta\right) \chi^{[2]} + \bar{c}_1, \tag{5}$$

where $\bar{c}_1 \equiv \bar{c}_1(t, \mathbf{x}, \boldsymbol{\tau}(t)) = \phi^{-1} \langle c_1 \rangle_Y$, and $\boldsymbol{\chi}^{[1]}$ and $\chi^{[2]}$ are closure variables. The resulting homogenized equation is written as

$$\phi \frac{\partial \langle c \rangle_Y}{\partial t} + \mathbf{U}\left(\langle c \rangle_Y\right) \cdot \nabla_{\mathbf{x}} \langle c \rangle_Y - \nabla_{\mathbf{x}} \cdot \left(\mathbf{D} \cdot \nabla_{\mathbf{x}} \langle c \rangle_Y\right) + \mathscr{R}\left(\langle c \rangle_Y\right) \left(\langle c \rangle_Y^2 - \phi^2 \theta\right) = \mathcal{O}\left(\epsilon\right) \quad \text{for } \mathbf{x} \in \Omega, \tag{6a}$$

where the effective parameters are defined as

$$\mathbf{U}\left(\langle c \rangle_Y\right) = \mathrm{Pe} \langle \mathbf{u} \rangle_Y + 2\phi^{-1} \langle c \rangle_Y \left[\phi \mathrm{Da} \frac{|\Gamma|}{|\mathcal{B}|} \langle \boldsymbol{\chi}^{[1]} \rangle_\Gamma - D \langle \nabla_{\boldsymbol{\xi}} \chi^{[2]} \rangle_Y + \mathrm{Pe} \epsilon \langle \mathbf{u} \chi^{[2]} \rangle_Y\right], \tag{6b}$$

$$\mathbf{D} = \phi D \mathbf{I} + D \langle \nabla_{\boldsymbol{\xi}} \boldsymbol{\chi}^{[1]} \rangle_Y - \mathrm{Pe} \epsilon \langle \mathbf{u} \otimes \boldsymbol{\chi}^{[1]} \rangle_Y, \tag{6c}$$

$$\mathscr{R}\left(\langle c \rangle_Y\right) = \mathrm{Da} \frac{|\Gamma|}{|\mathcal{B}|} \left[\epsilon^{-1} + 2\phi^{-1} \langle c \rangle_Y \langle \chi^{[2]} \rangle_\Gamma\right]. \tag{6d}$$

To calculate the closure variables found in system (6), Symbolica provides the closure problems

$$\mathrm{Pe} \epsilon \left(\mathbf{u}_0 - \langle \mathbf{u}_0 \rangle_{\mathcal{B}}\right) + \mathrm{Pe} \epsilon \mathbf{u}_0 \cdot \nabla_{\boldsymbol{\xi}} \boldsymbol{\chi}^{[1]} - D \nabla_{\boldsymbol{\xi}} \cdot \left(\mathbf{I} + \nabla_{\boldsymbol{\xi}} \boldsymbol{\chi}^{[1]}\right) = \mathbf{0} \quad \text{for } \boldsymbol{\xi} \in \mathcal{B}, \tag{7a}$$

subject to

$$-\mathbf{n} \cdot D \left(\mathbf{I} + \nabla_{\boldsymbol{\xi}} \boldsymbol{\chi}^{[1]}\right) = \mathbf{0} \quad \text{for } \boldsymbol{\xi} \in \Gamma, \tag{7b}$$

and

$$-\mathrm{Da} \frac{|\Gamma|}{|\mathcal{B}|} + \mathrm{Pe} \epsilon \mathbf{u}_0 \cdot \nabla_{\boldsymbol{\xi}} \chi^{[2]} - D \nabla_{\boldsymbol{\xi}}^2 \chi^{[2]} = 0 \quad \text{for } \boldsymbol{\xi} \in \mathcal{B}, \tag{8a}$$

subject to

$$-\mathbf{n} \cdot D \nabla_{\boldsymbol{\xi}} \chi^{[2]} = \mathrm{Da} \quad \text{for } \boldsymbol{\xi} \in \Gamma, \tag{8b}$$

where $\langle \boldsymbol{\chi}^{[1]} \rangle_{\mathcal{B}} = \mathbf{0}$ and $\langle \chi^{[2]} \rangle_{\mathcal{B}} = 0$.

As demonstrated, Symbolica quickly homogenized the system by following the algorithmic procedure for implementing the generalized closure form strategy. We note that the resulting homogenized equation and effective parameters are similar to those obtained in the first problem of Part 1 (i.e., system (19*))

Table 1. The simulation and mesh parameters used to solve the various models and problems defined on the pore-scale, unit-cell, and continuum domains for the single species system undergoing a nonlinear heterogeneous reaction. Here, $\mathbf{e}_x$ and $\mathbf{e}_\xi$ are the unit vectors in the x-direction and ξ-direction, respectively.

Simulation and Mesh Parameters
General Parameters
$\epsilon = 0.1, \quad D = 1, \quad \mathrm{Pe} = \epsilon^{-1}, \quad \mathrm{Da} = \epsilon^{0}, \quad \theta = \epsilon^{0}$
Pore-scale Fluid Flow and Mass Transport
$r_\epsilon = 0.02, \quad A_\epsilon = \epsilon^2, \quad \Phi_\epsilon = 8\mathbf{e}_x, \quad N_{elem} = 38351, \quad \max(\Delta x) = 0.0036, \quad \Delta t = 10^{-7}$
Homogenized Mass Transport
$\phi = 0.8744, \quad N_{elem} = 4006, \quad \max(\Delta x) = 0.0113, \quad \Delta t = 10^{-6}$
Unit-cell Fluid Flow and Closure Problems
$r = 0.2, \quad A = 1, \quad \Phi = 8\mathbf{e}_\xi, \quad N_{elem} = 44413, \quad \max(\Delta \xi) = 0.0099$

due to the similar microscopic system considered; however, the nonlinear heterogeneous reaction of the current system adds additional complexity to the homogenized results. The form of the current homogenized equation (equation (6a)) differs from that of the first problem in Part 1 by the effective reaction term $\mathscr{R}(\langle c\rangle_Y)(\langle c\rangle_Y^2 - \phi^2\theta)$, which emulates the nonlinear heterogeneous reaction. Additionally, the effective velocity $\mathbf{U}(\langle c\rangle_Y)$ and effective reaction rate $\mathscr{R}(\langle c\rangle_Y)$ have become dependent on the averaged concentration, $\langle c\rangle_Y$ (equations (6b) and (6d)). More specifically, the contributions in $\mathbf{U}(\langle c\rangle_Y)$ and $\mathscr{R}(\langle c\rangle_Y)$ due to the moderate reaction rate, which were discussed in the first problem of Part 1, are multiplied by $2\phi^{-1}\langle c\rangle_Y$. This creates a cubic nonlinearity in the effective reaction term and causes the effective advection term $\mathbf{U}(\langle c\rangle_Y)\cdot\nabla_{\mathbf{x}}\langle c\rangle_Y$, which does not vanish for $\mathrm{Pe} = 0$, to be nonlinear. This further illustrates how the forms of homogenized systems can be nontrivial, especially when nonlinearities are involved.

Finally, we note that the upscaled advection term can also be written as

$$\mathbf{U}\left(\langle c\rangle_Y\right)\cdot\nabla_{\mathbf{x}}\langle c\rangle_Y = \mathrm{Pe}\langle\mathbf{u}\rangle_Y\cdot\nabla_{\mathbf{x}}\langle c\rangle_Y + \phi^{-1}\mathbf{U}^*\cdot\nabla_{\mathbf{x}}\left(\langle c\rangle_Y^2\right), \tag{9a}$$

where

$$\mathbf{U}^* = \phi\mathrm{Da}\frac{|\Gamma|}{|\mathcal{B}|}\langle\boldsymbol{\chi}^{[1]}\rangle_\Gamma - D\langle\nabla_{\boldsymbol{\xi}}\chi^{[2]}\rangle_Y + \mathrm{Pe}\epsilon\langle\mathbf{u}\chi^{[2]}\rangle_Y. \tag{9b}$$

Here, $\mathbf{U}^*$ is identical to the contribution from the moderate reaction rate to the effective velocity discussed in the first problem of Part 1. As shown in equation (9a), the effective advection term has two contributions: (i) the common effective advection term $\mathrm{Pe}\langle\mathbf{u}\rangle_Y\cdot\nabla_{\mathbf{x}}\langle c\rangle_Y$ and (ii) the contribution from the moderate reaction rate $\phi^{-1}\mathbf{U}^*\cdot\nabla_{\mathbf{x}}(\langle c\rangle_Y^2)$. The second contribution has a similar form to an advection term, but the gradient is applied to $\langle c\rangle_Y^2$, which has its origins in the nonlinear heterogeneous reaction term. This provides insight on how different forms of heterogeneous reactions might affect homogenized systems in moderately reactive regimes.

3.2 Numerical Validation

3.2.1 Problem Setup

We now validate the homogenized model (systems (6), (7), and (8)) by numerically resolving and comparing its solution to the averaged solution from the pore-scale model (system (2)). Similar to Part 1, we use FEniCS (Logg et al., 2012; Alnaes et al., 2015) to resolve the models on the pore-scale, unit-cell, and continuum domains found in Figure 1*, which consider a 2D array of cylinders geometry. The geometric specifications for each domain are outlined in Table 1*, and details regarding the spatial and temporal discretizations are found in Table 1 with other simulation parameters.

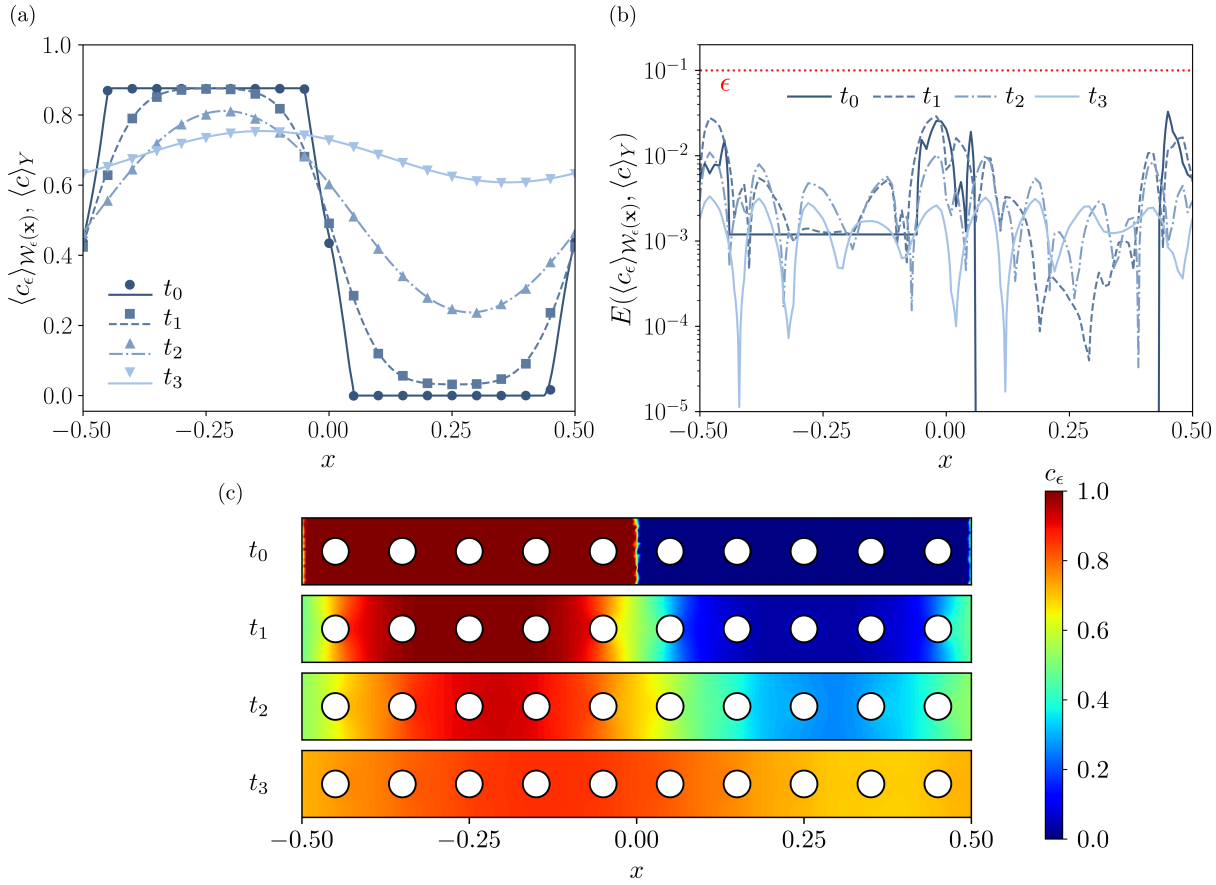

Figure 2. The numerical results for the system involving a single species undergoing a nonlinear heterogeneous reaction. (a) The $\mathcal{W}_\epsilon(\mathbf{x})$-averaged and Y-averaged concentration profiles from the pore-scale (symbols) and homogenized (lines) models, respectively, at various times along the x-direction. (b) The absolute error between the averaged concentration profiles of $\langle c_\epsilon \rangle_{\mathcal{W}_\epsilon(\mathbf{x})}$ and $\langle c \rangle_Y$ at various times along the x-direction. The upper error limit predicted by the homogenized model is displayed by the red dotted line. (c) Contour plots of the pore-scale concentration field c_ϵ at various times. Here, $t_0 = 0$, $t_1 = 0.25 \times 10^{-2}$, $t_2 = 1.25 \times 10^{-2}$, and $t_3 = 3.75 \times 10^{-2}$.

Regarding the initial conditions, we consider the same discontinuous concentration profile in the pore-scale simulation as assumed in the first problem of Part 1. Again, we note that the corresponding initial condition for the homogenized model is obtained by averaging the pore-scale initial condition using equation (22a*). We refer to Table 3* in Part 1 for further details regarding the initial conditions and boundary conditions used in the current problem.

Due to the identical geometric specifications, simulation parameters, initial conditions, boundary conditions, and closure problems between the first problem of Part 1 and the current problem, we reuse the flow field and closure problem solutions obtained from the previous problem. Therefore, we note that the flow velocity field, pressure field, and closure variable contours in the unit-cell domain can be found in Figure 2*.

3.2.2 Pore-scale and Homogenized Model Results

Upon solving the pore-scale (system (2)) and homogenized (systems (6), (7), and (8)) models, the pore-scale solution c_ϵ is averaged using the operator in equation (22a*) to obtain the averaged pore-scale solution $\langle c_\epsilon \rangle_{\mathcal{W}_\epsilon(\mathbf{x})}$. The absolute error between the averaged pore-scale solution and the respective homogenized solution $\langle c \rangle_Y$ is then calculated using equation (24*).

Similar to before, the pore-scale, averaged pore-scale, and homogenized model results are presented in Figure 2. The qualitative comparison in Figure 2(a) shows matching profiles of $\langle c_\epsilon \rangle_{\mathcal{W}_\epsilon(\mathbf{x})}$ and $\langle c \rangle_Y$ along the x-direction at the recorded times. As previously discussed, we note that the profiles in Figure 2(a)

are independent of y, and the initial condition of the homogenized model (displayed at $t = t_0$) shows a sharp slope around $x = 0$ due to the averaging of the discontinuous pore-scale initial condition.

To support the qualitative comparison, Figure 2(b) shows the absolute error between $\langle c_\epsilon \rangle_{\mathcal{W}_\epsilon(\mathbf{x})}$ and $\langle c \rangle_Y$ along the x-direction calculated using equation (24*). As shown, the error remains below the upper error limit denoted by the red dotted line for all times. This provides confidence in both the validity of the generalized closure form strategy for handling nonlinear problems and in the algorithmic procedure encoded in Symbolica.

Finally, contours of the pore-scale solution at various times are found in Figure 2(c). Similar to the contours from the first problem in Part 1, the initial discontinuous concentration profile seen at $t = t_0$ is quickly eliminated due to diffusive effects by $t = t_1$. In the contour at $t = t_2$, advective effects are observed to translate the diffused concentration profile downstream. As the system evolves further, the concentration profile advances towards a spatially-uniform steady-state at $t = t_3$.

With the qualitative and quantitative agreement between $\langle c_\epsilon \rangle_{\mathcal{W}_\epsilon(\mathbf{x})}$ and $\langle c \rangle_Y$ in Figure 2, we build confidence in Symbolica's encoding of the generalized closure form strategy. As previously discussed, our algorithm enables Symbolica to define valid, nontrivial closure forms and closure problems based on the considered system with no human interaction. Evidence of this is provided in equation (5), where the closure form generated by Symbolica includes the nonlinearity c_0^2. In subsurface engineering applications, geological systems with realistic complexities may experience a variety of reaction networks and physical regimes. Considering the diverse set of possible scenarios, where closure forms are likely to be unknown *a priori*, we find our algorithm invaluable for saving time and effort during the upscaling of such systems. In the next example problem, we use Symbolica to homogenize a complex, multi-component system undergoing multiple linear and nonlinear, homogeneous and heterogeneous reactions in the moderately reactive regime. We demonstrate that our framework can handle such complexities and automatically formulate the nontrivial closure forms and closure problems required for homogenization.

4 Nonlinear Homogeneous and Heterogeneous Reactions: Multiple Species

We now use Symbolica to homogenize a multi-species system undergoing linear and nonlinear, homogeneous and heterogeneous reactions with multiple reactive interfaces to demonstrate a complex implementation of the generalized closure form strategy via automated upscaling. The model reactive system we consider is written as

$$A + B \rightleftharpoons C \quad \text{in } \hat{\mathcal{B}}_\epsilon, \tag{10a}$$

$$B + M \to A + C \quad \text{in } \hat{\mathcal{B}}_\epsilon, \tag{10b}$$

$$C \rightleftharpoons G \quad \text{on } \hat{\Gamma}_\epsilon^{(1)} \cup \hat{\Gamma}_\epsilon^{(2)}, \tag{10c}$$

$$A + C \rightleftharpoons F \quad \text{on } \hat{\Gamma}_\epsilon^{(1)}, \tag{10d}$$

$$M \rightleftharpoons H \quad \text{on } \hat{\Gamma}_\epsilon^{(1)} \cup \hat{\Gamma}_\epsilon^{(3)} \cup \hat{\Gamma}_\epsilon^{(4)}, \tag{10e}$$

$$B + M \rightleftharpoons J \quad \text{on } \hat{\Gamma}_\epsilon^{(2)} \cup \hat{\Gamma}_\epsilon^{(3)} \cup \hat{\Gamma}_\epsilon^{(4)}, \tag{10f}$$

$$A \rightleftharpoons L \quad \text{on } \hat{\Gamma}_\epsilon^{(1)} \cup \hat{\Gamma}_\epsilon^{(2)} \cup \hat{\Gamma}_\epsilon^{(4)}, \tag{10g}$$

where each letter represents a unique species. To write the partial differential equations for the reaction network from system (4*), we let $N = 4$ and $N_\Gamma = 4$, such that

$$\frac{\partial \hat{c}_\epsilon^{(i)}}{\partial \hat{t}} + \hat{\nabla} \cdot \left(\hat{\mathbf{u}}_\epsilon \hat{c}_\epsilon^{(i)} - \hat{D}^{(i)} \hat{\nabla} \hat{c}_\epsilon^{(i)} \right) = \hat{R}_\epsilon^{(i)} \quad \text{in } \hat{\mathcal{B}}_\epsilon, \tag{11a}$$

subject to

$$-\mathbf{n}^{(j)} \cdot \hat{D}^{(i)} \hat{\nabla} \hat{c}_\epsilon^{(i)} = \hat{T}_\epsilon^{(i,j)} \quad \text{on } \hat{\Gamma}_\epsilon^{(j)}, \tag{11b}$$

where $i \in \mathbb{M} = \{m \in \mathbb{Z}^+ : m \leq 4\}$, $j \in \mathbb{M}$, and superscripts "(1)", "(2)", "(3)", and "(4)" correspond to species A, B, C, and M, respectively. The other letters correspond to species that exist on the reactive interfaces. Here, we define $\hat{R}_\epsilon^{(i)}$ as

$$\hat{R}_\epsilon^{(1)} = -\hat{\mathcal{K}}_{NL}^{(1,2)} \hat{c}_\epsilon^{(1)} \hat{c}_\epsilon^{(2)} + \hat{\mathcal{K}}_L^{(3)} \hat{c}_\epsilon^{(3)} + \hat{\mathcal{K}}_{NL}^{(2,4)} \hat{c}_\epsilon^{(2)} \hat{c}_\epsilon^{(4)}, \tag{11c}$$

$$\hat{R}_\epsilon^{(2)} = -\hat{\mathcal{K}}_{NL}^{(1,2)} \hat{c}_\epsilon^{(1)} \hat{c}_\epsilon^{(2)} + \hat{\mathcal{K}}_L^{(3)} \hat{c}_\epsilon^{(3)} - \hat{\mathcal{K}}_{NL}^{(2,4)} \hat{c}_\epsilon^{(2)} \hat{c}_\epsilon^{(4)}, \tag{11d}$$

$$\hat{R}_\epsilon^{(3)} = \hat{\mathcal{K}}_{NL}^{(1,2)} \hat{c}_\epsilon^{(1)} \hat{c}_\epsilon^{(2)} - \hat{\mathcal{K}}_L^{(3)} \hat{c}_\epsilon^{(3)} + \hat{\mathcal{K}}_{NL}^{(2,4)} \hat{c}_\epsilon^{(2)} \hat{c}_\epsilon^{(4)}, \tag{11e}$$

$$\hat{R}_\epsilon^{(4)} = -\hat{\mathcal{K}}_{NL}^{(2,4)} \hat{c}_\epsilon^{(2)} \hat{c}_\epsilon^{(4)}, \tag{11f}$$

where, considering equation (4b*), $p_L^{(i,j)}$ and $p_{NL}^{(i,j,k)}$ have been chosen accordingly and we have used the simplified notations $\hat{\mathcal{K}}_{NL}^{(n,2,4)} = \hat{\mathcal{K}}_{NL}^{(2,4)}$ for $n \in \{1,2,3,4\}$ and $\hat{\mathcal{K}}_{NL}^{(n,1,2)} = \hat{\mathcal{K}}_{NL}^{(1,2)}$ for $n \in \{1,2,3\}$. We also define $\hat{T}_\epsilon^{(i,j)}$ as

$$\hat{T}_\epsilon^{(1,1)} = \hat{\mathcal{K}}_{SL}^{(1,S)} \left(\hat{c}_\epsilon^{(1)} - \hat{C}_{SL}^{(1,S)} \right) + \hat{\mathcal{K}}_{SNL}^{(1,3,S)} \left(\hat{c}_\epsilon^{(1)} \hat{c}_\epsilon^{(3)} - \hat{C}_{SNL}^{(1,3,S)^2} \right), \tag{11g}$$

$$\hat{T}_\epsilon^{(1,n)} = \hat{\mathcal{K}}_{SL}^{(1,S)} \left(\hat{c}_\epsilon^{(1)} - \hat{C}_{SL}^{(1,S)} \right) \quad \text{for } n \in \{2,4\}, \tag{11h}$$

$$\hat{T}_\epsilon^{(2,n)} = \hat{\mathcal{K}}_{SNL}^{(2,4,S)} \left(\hat{c}_\epsilon^{(2)} \hat{c}_\epsilon^{(4)} - \hat{C}_{SNL}^{(2,4,S)^2} \right) \quad \text{for } n \in \{2,3,4\}, \tag{11i}$$

$$\hat{T}_\epsilon^{(3,1)} = \hat{\mathcal{K}}_{SL}^{(3,S)} \left(\hat{c}_\epsilon^{(3)} - \hat{C}_{SL}^{(3,S)} \right) + \hat{\mathcal{K}}_{SNL}^{(1,3,S)} \left(\hat{c}_\epsilon^{(1)} \hat{c}_\epsilon^{(3)} - \hat{C}_{SNL}^{(1,3,S)^2} \right), \tag{11j}$$

$$\hat{T}_\epsilon^{(3,2)} = \hat{\mathcal{K}}_{SL}^{(3,S)} \left(\hat{c}_\epsilon^{(3)} - \hat{C}_{SL}^{(3,S)} \right), \tag{11k}$$

$$\hat{T}_\epsilon^{(4,1)} = \hat{\mathcal{K}}_{SL}^{(4,S)} \left(\hat{c}_\epsilon^{(4)} - \hat{C}_{SL}^{(4,S)} \right), \tag{11l}$$

$$\hat{T}_\epsilon^{(4,2)} = \hat{\mathcal{K}}_{SNL}^{(2,4,S)} \left(\hat{c}_\epsilon^{(2)} \hat{c}_\epsilon^{(4)} - \hat{C}_{SNL}^{(2,4,S)^2} \right), \tag{11m}$$

$$\hat{T}_\epsilon^{(4,n)} = \hat{\mathcal{K}}_{SL}^{(4,S)} \left(\hat{c}_\epsilon^{(4)} - \hat{C}_{SL}^{(4,S)} \right) + \hat{\mathcal{K}}_{SNL}^{(2,4,S)} \left(\hat{c}_\epsilon^{(2)} \hat{c}_\epsilon^{(4)} - \hat{C}_{SNL}^{(2,4,S)^2} \right) \quad \text{for } n \in \{3,4\}, \tag{11n}$$

$$\hat{T}_\epsilon^{(m,n)} = 0 \quad \text{for } (m,n) \in \{(1,3),(2,1),(3,3),(3,4)\}, \tag{11o}$$

where again, $p_{SL}^{(i,j,k)}$ and $p_{SNL}^{(i,j,k,l)}$ from equation (4d*) have been chosen accordingly and the following simplified notations have been made: $\{\hat{\mathcal{K}}_{SL}^{(1,n,1)}, \hat{C}_{SL}^{(1,n,1)}\} = \{\hat{\mathcal{K}}_{SL}^{(1,S)}, \hat{C}_{SL}^{(1,S)}\}$ for $n \in \{1,2,4\}$, $\{\hat{\mathcal{K}}_{SNL}^{(m,1,1,3)}, \hat{C}_{SNL}^{(m,1,1,3)}\} = \{\hat{\mathcal{K}}_{SNL}^{(1,3,S)}, \hat{C}_{SNL}^{(1,3,S)}\}$ for $m \in \{1,3\}$, $\{\hat{\mathcal{K}}_{SNL}^{(m,n,2,4)}, \hat{C}_{SNL}^{(m,n,2,4)}\} = \{\hat{\mathcal{K}}_{SNL}^{(2,4,S)}, \hat{C}_{SNL}^{(2,4,S)}\}$ for $m \in \{2,4\}$ and $n \in \{2,3,4\}$, $\{\hat{\mathcal{K}}_{SL}^{(3,n,3)}, \hat{C}_{SL}^{(3,n,3)}\} = \{\hat{\mathcal{K}}_{SL}^{(3,S)}, \hat{C}_{SL}^{(3,S)}\}$ for $n \in \{1,2\}$, $\{\hat{\mathcal{K}}_{SL}^{(4,n,4)}, \hat{C}_{SL}^{(4,n,4)}\} = \{\hat{\mathcal{K}}_{SL}^{(4,S)}, \hat{C}_{SL}^{(4,S)}\}$ for $n \in \{1,3,4\}$.

Using the scales defined in equation (5*) while letting $\hat{\mathcal{C}}^{(i)} = \hat{\mathcal{C}}^{(*)}$, Symbolica obtains the dimensionless system

$$\frac{\partial c_\epsilon^{(i)}}{\partial t} + \nabla \cdot \left(\mathrm{Pe}\mathbf{u}_\epsilon c_\epsilon^{(i)} - D^{(i)} \nabla c_\epsilon^{(i)} \right) = R_\epsilon^{(i)} \quad \text{in } \mathcal{B}_\epsilon, \tag{12a}$$

subject to

$$-\mathbf{n}^{(j)} \cdot D^{(i)} \nabla c_\epsilon^{(i)} = T_\epsilon^{(i,j)} \quad \text{on } \Gamma_\epsilon^{(j)}, \tag{12b}$$

where $\hat{R}_\epsilon^{(i)}$ is defined as

$$R_\epsilon^{(1)} = -\mathrm{Da}_1 c_\epsilon^{(1)} c_\epsilon^{(2)} + \mathrm{Da}_2 c_\epsilon^{(3)} + \mathrm{Da}_3 c_\epsilon^{(2)} c_\epsilon^{(4)}, \tag{12c}$$

$$R_\epsilon^{(2)} = -\mathrm{Da}_1 c_\epsilon^{(1)} c_\epsilon^{(2)} + \mathrm{Da}_2 c_\epsilon^{(3)} - \mathrm{Da}_3 c_\epsilon^{(2)} c_\epsilon^{(4)}, \tag{12d}$$

$$R_\epsilon^{(3)} = \mathrm{Da}_1 c_\epsilon^{(1)} c_\epsilon^{(2)} - \mathrm{Da}_2 c_\epsilon^{(3)} + \mathrm{Da}_3 c_\epsilon^{(2)} c_\epsilon^{(4)}, \tag{12e}$$

$$R_\epsilon^{(4)} = -\mathrm{Da}_3 c_\epsilon^{(2)} c_\epsilon^{(4)}, \tag{12f}$$

and $T_\epsilon^{(i,j)}$ is defined as

$$T_\epsilon^{(1,1)} = \mathrm{Da}_4 \left(c_\epsilon^{(1)} - \theta_1 \right) + \mathrm{Da}_5 \left(c_\epsilon^{(1)} c_\epsilon^{(3)} - \theta_2 \right), \tag{12g}$$

$$T_\epsilon^{(1,n)} = \mathrm{Da}_4 \left(c_\epsilon^{(1)} - \theta_1 \right) \quad \text{for } n \in \{2, 4\}, \tag{12h}$$

$$T_\epsilon^{(2,n)} = \mathrm{Da}_8 \left(c_\epsilon^{(2)} c_\epsilon^{(4)} - \theta_5 \right) \quad \text{for } n \in \{2, 3, 4\}, \tag{12i}$$

$$T_\epsilon^{(3,1)} = \mathrm{Da}_6 \left(c_\epsilon^{(3)} - \theta_3 \right) + \mathrm{Da}_5 \left(c_\epsilon^{(1)} c_\epsilon^{(3)} - \theta_2 \right), \tag{12j}$$

$$T_\epsilon^{(3,2)} = \mathrm{Da}_6 \left(c_\epsilon^{(3)} - \theta_3 \right), \tag{12k}$$

$$T_\epsilon^{(4,1)} = \mathrm{Da}_7 \left(c_\epsilon^{(4)} - \theta_4 \right), \tag{12l}$$

$$T_\epsilon^{(4,2)} = \mathrm{Da}_8 \left(c_\epsilon^{(2)} c_\epsilon^{(4)} - \theta_5 \right), \tag{12m}$$

$$T_\epsilon^{(4,n)} = \mathrm{Da}_7 \left(c_\epsilon^{(4)} - \theta_4 \right) + \mathrm{Da}_8 \left(c_\epsilon^{(2)} c_\epsilon^{(4)} - \theta_5 \right) \quad \text{for } n \in \{3, 4\}, \tag{12n}$$

$$T_\epsilon^{(m,n)} = 0 \quad \text{for } (m,n) \in \{(1,3), (2,1), (3,3), (3,4)\}. \tag{12o}$$

Here, Symbolica defines the Péclet number, 8 Damköhler numbers, and 5 concentration ratios as

$$\begin{gathered}
\mathrm{Pe}=\frac{\hat{\mathcal{U}}\hat{\mathcal{L}}}{\hat{\mathcal{D}}},\quad \mathrm{Da}_1=\frac{\hat{\mathcal{K}}_{NL}^{(1,2)}\hat{\mathcal{L}}^2\hat{\mathcal{C}}^{(*)}}{\hat{\mathcal{D}}},\quad \mathrm{Da}_2=\frac{\hat{\mathcal{K}}_{L}^{(3)}\hat{\mathcal{L}}^2}{\hat{\mathcal{D}}},\quad \mathrm{Da}_3=\frac{\hat{\mathcal{K}}_{NL}^{(2,4)}\hat{\mathcal{L}}^2\hat{\mathcal{C}}^{(*)}}{\hat{\mathcal{D}}},\quad \mathrm{Da}_4=\frac{\hat{\mathcal{K}}_{SL}^{(1,S)}\hat{\mathcal{L}}}{\hat{\mathcal{D}}},\\
\mathrm{Da}_5=\frac{\hat{\mathcal{K}}_{SNL}^{(1,3,S)}\hat{\mathcal{L}}\hat{\mathcal{C}}^{(*)}}{\hat{\mathcal{D}}},\quad \mathrm{Da}_6=\frac{\hat{\mathcal{K}}_{SL}^{(3,S)}\hat{\mathcal{L}}}{\hat{\mathcal{D}}},\quad \mathrm{Da}_7=\frac{\hat{\mathcal{K}}_{SL}^{(4,S)}\hat{\mathcal{L}}}{\hat{\mathcal{D}}},\quad \mathrm{Da}_8=\frac{\hat{\mathcal{K}}_{SNL}^{(2,4,S)}\hat{\mathcal{L}}\hat{\mathcal{C}}^{(*)}}{\hat{\mathcal{D}}},\\
\theta_1=\frac{\hat{C}_{SL}^{(1,S)}}{\hat{\mathcal{C}}^{(*)}},\quad \theta_2=\frac{\hat{C}_{SNL}^{(1,3,S)^2}}{\hat{\mathcal{C}}^{(*)^2}},\quad \theta_3=\frac{\hat{C}_{SL}^{(3,S)}}{\hat{\mathcal{C}}^{(*)}},\quad \theta_4=\frac{\hat{C}_{SL}^{(4,S)}}{\hat{\mathcal{C}}^{(*)}},\quad \theta_5=\frac{\hat{C}_{SNL}^{(2,4,S)^2}}{\hat{\mathcal{C}}^{(*)^2}}.
\end{gathered}\tag{13}$$

To trigger the implementation of the generalized closure form strategy in Symbolica, we study a moderately reactive scenario where diffusive and heterogeneous reactive terms are of similar order. We also consider high advection and fast homogeneous reactions by letting Pe, Da_1, Da_2, and Da_3 be of order $\mathcal{O}(\epsilon^{-1})$, and all other dimensionless numbers (i.e., Da_n for $n>3$ and all concentration ratios) be of order $\mathcal{O}(\epsilon^0)$.

4.1 Homogenized Results

The total execution time for Symbolica to homogenize system (12) for $\langle c^{(i)}\rangle_Y=\langle c_0^{(i)}\rangle_Y+\epsilon\langle c_1^{(i)}\rangle_Y+\mathcal{O}(\epsilon^2)$, where $i\in\{1,2,3,4\}$, with $\mathcal{O}(\epsilon)$ error was 11 minutes. As compared with the previous problem, the increase in homogenization time is due to the increase in system complexity. The closure forms Symbolica generated are written as

$$c_1^{(1)}=\chi^{(1)[1]}+\chi^{(1)[2]}c_0^{(1)}+\chi^{(1)[3]}c_0^{(1)}c_0^{(3)}+\boldsymbol{\chi}^{(1)[4]}\cdot\nabla_{\mathbf{x}}c_0^{(1)}+\overline{c}_1^{(1)},\tag{14a}$$

$$c_1^{(2)}=\chi^{(2)[1]}\left(c_0^{(2)}c_0^{(4)}-\theta_5\right)+\boldsymbol{\chi}^{(2)[2]}\cdot\nabla_{\mathbf{x}}c_0^{(2)}+\overline{c}_1^{(2)},\tag{14b}$$

$$c_1^{(3)}=\chi^{(3)[1]}+\chi^{(3)[2]}c_0^{(3)}+\chi^{(3)[3]}c_0^{(1)}c_0^{(3)}+\boldsymbol{\chi}^{(3)[4]}\cdot\nabla_{\mathbf{x}}c_0^{(3)}+\overline{c}_1^{(3)},\tag{14c}$$

$$c_1^{(4)}=\chi^{(4)[1]}+\chi^{(4)[2]}c_0^{(4)}+\chi^{(4)[3]}c_0^{(2)}c_0^{(4)}+\boldsymbol{\chi}^{(4)[4]}\cdot\nabla_{\mathbf{x}}c_0^{(4)}+\overline{c}_1^{(4)},\tag{14d}$$

where $\overline{c}_1^{(i)}\equiv\overline{c}_1^{(i)}(t,\mathbf{x},\boldsymbol{\tau}(t))=\phi^{-1}\langle c_1^{(i)}\rangle_Y$, and $\boldsymbol{\chi}^{(i)[k_1]}$ and $\chi^{(i)[k_2]}$ are closure variables to $\langle c^{(i)}\rangle_Y$ where $\langle\boldsymbol{\chi}^{(i)[k_1]}\rangle_{\mathcal{B}}=\mathbf{0}$ and $\langle\chi^{(i)[k_2]}\rangle_{\mathcal{B}}=0$. Here, $k_1\in\{4\}$ and $k_2\in\{1,2,3\}$ for $i\in\{1,3,4\}$, and $k_1\in\{2\}$ and $k_2\in\{1\}$ for $i\in\{2\}$. The resulting homogenized system is written as

$$\begin{aligned}
&\phi^2\frac{\partial\langle c^{(1)}\rangle_Y}{\partial t}+\mathbf{U}^{(1)}\left(\langle c^{(3)}\rangle_Y\right)\cdot\nabla_{\mathbf{x}}\langle c^{(1)}\rangle_Y+\mathbf{V}^{(1)}\left(\langle c^{(1)}\rangle_Y\right)\cdot\nabla_{\mathbf{x}}\langle c^{(3)}\rangle_Y-\phi\nabla_{\mathbf{x}}\cdot\left(\mathbf{D}^{(1)}\cdot\nabla_{\mathbf{x}}\langle c^{(1)}\rangle_Y\right)\\
&+\mathscr{R}^{(1)}\left(\langle c^{(1)}\rangle_Y,\langle c^{(3)}\rangle_Y\right)=-\phi\mathrm{Da}_1\langle c^{(1)}\rangle_Y\langle c^{(2)}\rangle_Y+\phi^2\mathrm{Da}_2\langle c^{(3)}\rangle_Y+\phi\mathrm{Da}_3\langle c^{(2)}\rangle_Y\langle c^{(4)}\rangle_Y\quad\text{for }\mathbf{x}\in\Omega,
\end{aligned}\tag{15a}$$

$$\begin{aligned}
&\phi^2\frac{\partial\langle c^{(2)}\rangle_Y}{\partial t}+\mathbf{U}^{(2)}\left(\langle c^{(4)}\rangle_Y\right)\cdot\nabla_{\mathbf{x}}\langle c^{(2)}\rangle_Y+\mathbf{V}^{(2)}\left(\langle c^{(2)}\rangle_Y\right)\cdot\nabla_{\mathbf{x}}\langle c^{(4)}\rangle_Y-\phi\nabla_{\mathbf{x}}\cdot\left(\mathbf{D}^{(2)}\cdot\nabla_{\mathbf{x}}\langle c^{(2)}\rangle_Y\right)\\
&+\mathscr{R}^{(2)}\left(\langle c^{(2)}\rangle_Y,\langle c^{(4)}\rangle_Y\right)=-\phi\mathrm{Da}_1\langle c^{(1)}\rangle_Y\langle c^{(2)}\rangle_Y+\phi^2\mathrm{Da}_2\langle c^{(3)}\rangle_Y-\phi\mathrm{Da}_3\langle c^{(2)}\rangle_Y\langle c^{(4)}\rangle_Y\quad\text{for }\mathbf{x}\in\Omega,
\end{aligned}\tag{15b}$$

$$\begin{aligned}
&\phi^2\frac{\partial\langle c^{(3)}\rangle_Y}{\partial t}+\mathbf{U}^{(3)}\left(\langle c^{(1)}\rangle_Y\right)\cdot\nabla_{\mathbf{x}}\langle c^{(3)}\rangle_Y+\mathbf{V}^{(3)}\left(\langle c^{(3)}\rangle_Y\right)\cdot\nabla_{\mathbf{x}}\langle c^{(1)}\rangle_Y-\phi\nabla_{\mathbf{x}}\cdot\left(\mathbf{D}^{(3)}\cdot\nabla_{\mathbf{x}}\langle c^{(3)}\rangle_Y\right)\\
&+\mathscr{R}^{(3)}\left(\langle c^{(1)}\rangle_Y,\langle c^{(3)}\rangle_Y\right)=\phi\mathrm{Da}_1\langle c^{(1)}\rangle_Y\langle c^{(2)}\rangle_Y-\phi^2\mathrm{Da}_2\langle c^{(3)}\rangle_Y+\phi\mathrm{Da}_3\langle c^{(2)}\rangle_Y\langle c^{(4)}\rangle_Y\quad\text{for }\mathbf{x}\in\Omega,
\end{aligned}\tag{15c}$$

$$\begin{aligned}
&\phi^2\frac{\partial\langle c^{(4)}\rangle_Y}{\partial t}+\mathbf{U}^{(4)}\left(\langle c^{(2)}\rangle_Y\right)\cdot\nabla_{\mathbf{x}}\langle c^{(4)}\rangle_Y+\mathbf{V}^{(4)}\left(\langle c^{(4)}\rangle_Y\right)\cdot\nabla_{\mathbf{x}}\langle c^{(2)}\rangle_Y-\phi\nabla_{\mathbf{x}}\cdot\left(\mathbf{D}^{(4)}\cdot\nabla_{\mathbf{x}}\langle c^{(4)}\rangle_Y\right)\\
&+\mathscr{R}^{(4)}\left(\langle c^{(2)}\rangle_Y,\langle c^{(4)}\rangle_Y\right)=-\phi\mathrm{Da}_3\langle c^{(2)}\rangle_Y\langle c^{(4)}\rangle_Y\quad\text{for }\mathbf{x}\in\Omega,
\end{aligned}\tag{15d}$$

where $\mathbf{U}^{(1)}(\langle c^{(3)}\rangle_Y)$, $\mathbf{U}^{(2)}(\langle c^{(4)}\rangle_Y)$, $\mathbf{U}^{(3)}(\langle c^{(1)}\rangle_Y)$, and $\mathbf{U}^{(4)}(\langle c^{(2)}\rangle_Y)$ are the effective velocities, $\mathbf{V}^{(1)}(\langle c^{(1)}\rangle_Y)$, $\mathbf{V}^{(2)}(\langle c^{(2)}\rangle_Y)$, $\mathbf{V}^{(3)}(\langle c^{(3)}\rangle_Y)$, and $\mathbf{V}^{(4)}(\langle c^{(4)}\rangle_Y)$ are the effective parameters corresponding to the emergent terms, $\mathbf{D}^{(i)}$ are the dispersion tensors for $i \in \{1,2,3,4\}$, and $\mathscr{R}^{(1)}(\langle c^{(1)}\rangle_Y, \langle c^{(3)}\rangle_Y)$, $\mathscr{R}^{(2)}(\langle c^{(2)}\rangle_Y, \langle c^{(4)}\rangle_Y)$, $\mathscr{R}^{(3)}(\langle c^{(1)}\rangle_Y, \langle c^{(3)}\rangle_Y)$, and $\mathscr{R}^{(4)}(\langle c^{(2)}\rangle_Y, \langle c^{(4)}\rangle_Y)$ are effective reaction rates. While the effective parameter definitions for system (15) are recorded in Appendix A, the parameters for equation (15a) are reprinted here for discussion:

$$\begin{aligned}\mathbf{U}^{(1)}\left(\langle c^{(3)}\rangle_Y\right) = \phi \mathrm{Pe}\langle \mathbf{u}\rangle_Y + \phi^2 \frac{\mathrm{Da}_4}{|\mathcal{B}|}\left[|\Gamma^{(1)}|\langle \boldsymbol{\chi}^{(1)[4]}\rangle_{\Gamma^{(1)}} + |\Gamma^{(2)}|\langle \boldsymbol{\chi}^{(1)[4]}\rangle_{\Gamma^{(2)}} + |\Gamma^{(4)}|\langle \boldsymbol{\chi}^{(1)[4]}\rangle_{\Gamma^{(4)}}\right] \\ -\phi D^{(1)}\langle \nabla_{\boldsymbol{\xi}}\chi^{(1)[2]}\rangle_Y + \phi \mathrm{Pe}\epsilon\langle \mathbf{u}\chi^{(1)[2]}\rangle_Y \\ +\langle c^{(3)}\rangle_Y\left[\phi\frac{\mathrm{Da}_5}{|\mathcal{B}|}|\Gamma^{(1)}|\langle \boldsymbol{\chi}^{(1)[4]}\rangle_{\Gamma^{(1)}} - D^{(1)}\langle \nabla_{\boldsymbol{\xi}}\chi^{(1)[3]}\rangle_Y + \mathrm{Pe}\epsilon\langle \mathbf{u}\chi^{(1)[3]}\rangle_Y\right],\end{aligned} \tag{16a}$$

$$\mathbf{V}^{(1)}\left(\langle c^{(1)}\rangle_Y\right) = \langle c^{(1)}\rangle_Y\left[\phi\frac{\mathrm{Da}_5}{|\mathcal{B}|}|\Gamma^{(1)}|\langle \boldsymbol{\chi}^{(3)[4]}\rangle_{\Gamma^{(1)}} - D^{(1)}\langle \nabla_{\boldsymbol{\xi}}\chi^{(1)[3]}\rangle_Y + \mathrm{Pe}\epsilon\langle \mathbf{u}\chi^{(1)[3]}\rangle_Y\right], \tag{16b}$$

$$\mathbf{D}^{(1)} = \phi D^{(1)}\mathbf{I} + D^{(1)}\langle \nabla_{\boldsymbol{\xi}}\boldsymbol{\chi}^{(1)[4]}\rangle_Y - \mathrm{Pe}\epsilon\langle \mathbf{u}\otimes\boldsymbol{\chi}^{(1)[4]}\rangle_Y, \tag{16c}$$

$$\begin{aligned}\mathscr{R}^{(1)}\left(\langle c^{(1)}\rangle_Y, \langle c^{(3)}\rangle_Y\right) = \mathscr{R}_1^{(1)}\left[\phi^2\langle c^{(1)}\rangle_Y - \phi^3\theta_1\right] + \mathscr{R}_2^{(1)}\left[\phi\langle c^{(1)}\rangle_Y\langle c^{(3)}\rangle_Y - \phi^3\theta_2\right] \\ +\phi^3\mathscr{R}_3^{(1)} + \phi^2\mathscr{R}_4^{(1)}\langle c^{(1)}\rangle_Y + \phi^2\mathscr{R}_5^{(1)}\langle c^{(3)}\rangle_Y + \phi\mathscr{R}_6^{(1)}\langle c^{(1)}\rangle_Y\langle c^{(3)}\rangle_Y \\ +\mathscr{R}_7^{(1)}\left[\langle c^{(1)}\rangle_Y\right]^2\langle c^{(3)}\rangle_Y + \mathscr{R}_8^{(1)}\langle c^{(1)}\rangle_Y\left[\langle c^{(3)}\rangle_Y\right]^2,\end{aligned} \tag{16d}$$

where $\mathscr{R}_k^{(1)}$ are the coefficients of the effective reaction rate $\mathscr{R}^{(1)}(\langle c^{(1)}\rangle_Y, \langle c^{(3)}\rangle_Y)$ for $k \in \{1,2,3,4,5,6,7,8\}$, which are defined in Appendix B. We note that the effective parameters of the other equations are of similar forms. In total, Symbolica defined 14 different closure problems, recorded in Appendix C, to solve for the 14 closure variables.

As shown in system (14), the closure forms defined by Symbolica are nontrivial. Their generation and utilization to derive the 14 closure problems would create an arduous task if completed by hand. However, with our encoded algorithm, Symbolica formulated these entities in a reasonable amount of time with no human interaction, nor prior knowledge about the closure of the system.

While the equation forms in system (15) are similar to those found in the previous problems, with additional terms accounting for the homogeneous reactions, the effective parameters differ. As shown in system (16), the effective velocity $\mathbf{U}^{(1)}(\langle c^{(3)}\rangle_Y)$ adds a new coupling in the upscaled system due to its dependency on $\langle c^{(3)}\rangle_Y$, and the effective parameter of the emergent term $\mathbf{V}^{(1)}(\langle c^{(1)}\rangle_Y)$ induces a coupling due to its dependency on $\langle c^{(1)}\rangle_Y$. Similar couplings are induced by the other effective parameters recorded in Appendix A, and originate from the moderately-strong bimolecular heterogeneous reactions. Lastly, we note that within the complexities of the effective reaction rates, resemblances of the heterogeneous reactions can be found (e.g., equation (16d)).

4.2 Numerical Validation

4.2.1 Problem Setup

We again provide numerical validation by resolving and comparing the averaged solutions from the pore-scale (system (12)) and homogenized (system (15)) models. To conduct the validation, we consider a 2D array of cylinders with four different sizes in a Cartesian plane to accommodate the four considered interfaces of the problem. Schematics of the pore-scale, unit-cell, and continuum domains considered are shown in Figure 3 with relevant geometric labels, which are detailed in Table 2. The spatial and temporal discretizations to resolve the models in these domains are refined to show converged solutions to plotting accuracy, and further details regarding the discretizations of each mesh are presented with other simulation parameters in Table 3. Regarding the initial conditions, discontinuous concentration profiles, where the concentration is alternatively equal to 0 or 1 in different sections of the domain, are assumed in the

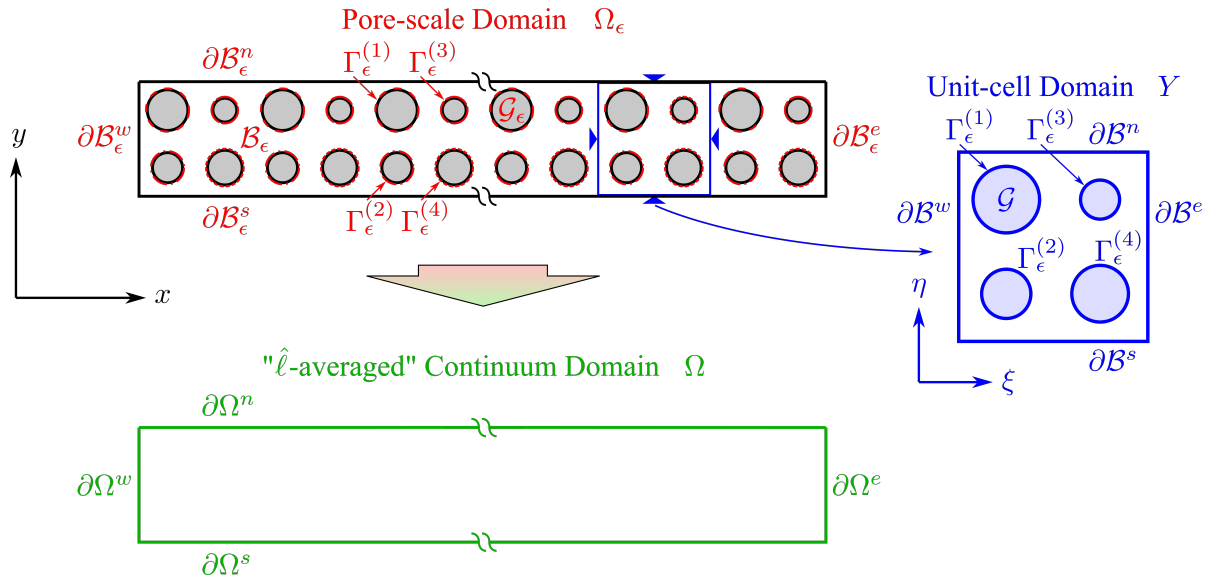

Figure 3. A schematic of the 2D pore-scale, unit-cell, and continuum domains considered for the four-cylinders geometry. Details of the labeled geometric aspects are found in Table 2.

pore-scale simulation, while the averaging operator in equation (22a*) is applied to the profiles to obtain the corresponding initial conditions for the homogenized model. Further details regarding simulation initial conditions and boundary conditions are provided in Table 4.

Similar to the first problem of Part 1, the fluid velocity and pressure fields for the pore-scale model are obtained by resolving system (6*) for $A_\epsilon = \epsilon^2$. Again, the flow is driven by representing the pressure gradient as $\nabla p_\epsilon = \Phi_\epsilon + \nabla\tilde{p}_\epsilon$, where Φ_ϵ is a known, large-scale pressure gradient across the pore-scale domain and $\nabla\tilde{p}_\epsilon$ is the gradient of an unknown local pressure field. With an appropriate value for Φ_ϵ, the flow fields $\mathbf{u}_\epsilon$ and $\tilde{p}_\epsilon$ are resolved such that $|\mathbf{u}_\epsilon| \sim \mathcal{O}(1)$, which verifies consistency between $\hat{\mathcal{U}}$ calculated using the definition of the Péclet number in equation (13) and the magnitude of the driven flow $|\mathbf{u}_\epsilon|$.

In the homogenized model, we again solve system (23*) for the flow field in the unit-cell domain using the values for A and Φ provided in Table 3. We note that the flow in the unit-cell domain should be reflective of that in the pore-scale domain, i.e. $\Phi = \Phi_\epsilon$. With the unit-cell flow fields, the average of the velocity field $\mathbf{u}$ over the unit-cell can be calculated and used as needed in the effective parameters and closure problems.

4.2.2 Flow and Closure Problem Results

Following the previous procedure, the fluid velocity and pressure fields are resolved in the pore-scale domain using system (6*), and in the unit-cell domain using system (23*). The resulting flow velocity magnitude $|\mathbf{u}|$ and local pressure $\tilde{p}$ contours in the unit-cell domain are plotted in Figures 4(a) and 4(b), respectively. We note that compared with the first problem of Part 1, larger values of Φ_ϵ and Φ were used to generate flow fields such that $|\mathbf{u}_\epsilon| \sim |\mathbf{u}| \sim \mathcal{O}(1)$, as the current geometry is more resistant to the fluid flow than the previous geometry. We also note that the flow fields in the pore-scale domain do not provide information beyond the flow fields in the unit-cell domain due to the periodic nature of the problem. Therefore, only the unit-cell flow fields are presented.

With the solution to the fluid flow problem, the 14 closure problems defined by Symbolica (Appendix C) are solved in the unit-cell domain. Contour plots of the closure solutions can be found in Appendix D.

Table 2. Specifications for the geometric aspects in the pore-scale, unit-cell, and continuum domains considering the 2D array of cylinders geometry with cylinders of four different sizes. Note that $\boldsymbol{\mathcal{X}}_\epsilon$, $\boldsymbol{\mathcal{Y}}_\epsilon$, $\boldsymbol{\mathcal{X}}$, and $\boldsymbol{\mathcal{Y}}$ are only used to consolidate the tabulated entries.

Variable	Definition for the 2D Array of Cylinders Geometry
	Dimensional Parameters
$\hat{\ell}$	Unit-cell domain length
$\hat{\mathcal{L}}$	Pore-scale domain length
$\hat{r}_\epsilon^{(j)}$	Cylinder radius for interface j
	Pore-scale Domain
$r_\epsilon^{(j)}$	$\hat{r}_\epsilon^{(j)}/\hat{\mathcal{L}} \quad \text{for } j \in \{1,2,3,4\}$
Ω_ϵ	$\{(x,y) : -0.5 < x < 0.5,\ -0.5\epsilon < y < 0.5\epsilon\}$
$\boldsymbol{\mathcal{X}}_\epsilon$	$[0.75,\ 0.75,\ 0.25,\ 0.25]$
$\boldsymbol{\mathcal{Y}}_\epsilon$	$[0.25,\ -0.25,\ 0.25,\ -0.25]$
$\mathcal{G}_\epsilon$	$\bigcup_{j=1}^{4}\{(x,y) : (x + 0.5 + [\boldsymbol{\mathcal{X}}_\epsilon]_j\,\epsilon - m\epsilon)^2 + (y - [\boldsymbol{\mathcal{Y}}_\epsilon]_j\,\epsilon)^2 < r_\epsilon^{(j)^2},\ m \in \mathbb{Z}^+,\ m \le \epsilon^{-1}\}$
$\Gamma_\epsilon^{(j)}$	$\{(x,y) : (x + 0.5 + [\boldsymbol{\mathcal{X}}_\epsilon]_j\,\epsilon - m\epsilon)^2 + (y - [\boldsymbol{\mathcal{Y}}_\epsilon]_j\,\epsilon)^2 = r_\epsilon^{(j)^2},\ m \in \mathbb{Z}^+,\ m \le \epsilon^{-1}\}$
Γ_ϵ	$\bigcup_{j=1}^{4}\Gamma_\epsilon^{(j)}$
$\mathcal{B}_\epsilon$	$\Omega_\epsilon \setminus (\mathcal{G}_\epsilon \cup \Gamma_\epsilon)$
$\partial\mathcal{B}_\epsilon^w$	$\{(x,y) : x = -0.5,\ -0.5\epsilon < y < 0.5\epsilon\}$
$\partial\mathcal{B}_\epsilon^e$	$\{(x,y) : x = 0.5,\ -0.5\epsilon < y < 0.5\epsilon\}$
$\partial\mathcal{B}_\epsilon^s$	$\{(x,y) : -0.5 < x < 0.5,\ y = -0.5\epsilon\}$
$\partial\mathcal{B}_\epsilon^n$	$\{(x,y) : -0.5 < x < 0.5,\ y = 0.5\epsilon\}$
	Unit-cell Domain
$r^{(j)}$	$\hat{r}_\epsilon^{(j)}/\hat{\ell} \quad \text{for } j \in \{1,2,3,4\}$
Y	$\{(\xi,\eta) : -0.5 < \xi < 0.5,\ -0.5 < \eta < 0.5\}$
$\boldsymbol{\mathcal{X}}$	$[0.25,\ 0.25,\ -0.25,\ -0.25]$
$\boldsymbol{\mathcal{Y}}$	$[0.25,\ -0.25,\ 0.25,\ -0.25]$
$\mathcal{G}$	$\bigcup_{j=1}^{4}\{(\xi,\eta) : (\xi - [\boldsymbol{\mathcal{X}}]_j)^2 + (\eta - [\boldsymbol{\mathcal{Y}}]_j)^2 < r^{(j)^2}\}$
$\Gamma^{(j)}$	$\{(\xi,\eta) : (\xi - [\boldsymbol{\mathcal{X}}]_j)^2 + (\eta - [\boldsymbol{\mathcal{Y}}]_j)^2 = r^{(j)^2}\}$
Γ	$\bigcup_{j=1}^{4}\Gamma^{(j)}$
$\mathcal{B}$	$\Omega \setminus (\mathcal{G} \cup \Gamma)$
$\partial\mathcal{B}^w$	$\{(\xi,\eta) : \xi = -0.5,\ -0.5 < \eta < 0.5\}$
$\partial\mathcal{B}^e$	$\{(\xi,\eta) : \xi = 0.5,\ -0.5 < \eta < 0.5\}$
$\partial\mathcal{B}^s$	$\{(\xi,\eta) : -0.5 < \xi < 0.5,\ \eta = -0.5\}$
$\partial\mathcal{B}^n$	$\{(\xi,\eta) : -0.5 < \xi < 0.5,\ \eta = 0.5\}$
$\lvert Y\rvert$	1
$\lvert\mathcal{G}\rvert$	$\sum_{j=1}^{4}\pi r^{(j)^2}$
$\lvert\Gamma^{(j)}\rvert$	$2\pi r^{(j)}$
$\lvert\Gamma\rvert$	$\sum_{j=1}^{4}\Gamma^{(j)}$
$\lvert\mathcal{B}\rvert$	$\lvert Y\rvert - \lvert\mathcal{G}\rvert$
ϕ	$\lvert\mathcal{B}\rvert \,/\, \lvert Y\rvert$
	"$\hat{\ell}$-averaged" Continuum Domain
Ω	$\{(x,y) : -0.5 < x < 0.5,\ -0.5\epsilon < y < 0.5\epsilon\}$
$\partial\Omega^w$	$\{(x,y) : x = -0.5,\ -0.5\epsilon < y < 0.5\epsilon\}$
$\partial\Omega^e$	$\{(x,y) : x = 0.5,\ -0.5\epsilon < y < 0.5\epsilon\}$
$\partial\Omega^s$	$\{(x,y) : -0.5 < x < 0.5,\ y = -0.5\epsilon\}$
$\partial\Omega^n$	$\{(x,y) : -0.5 < x < 0.5,\ y = 0.5\epsilon\}$

Table 3. The simulation and mesh parameters used to solve the various models and problems defined on the pore-scale, unit-cell, and continuum domains for the multi-species system undergoing linear and nonlinear, homogeneous and heterogeneous reactions. Here, $\mathbf{e}_x$ and $\mathbf{e}_\xi$ are the unit vectors in the x-direction and ξ-direction, respectively, $i \in \{1,2,3,4\}$, $k_1 \in \{1,2,3\}$, $k_2 \in \{4,5,6,7,8\}$, and $k_3 \in \{1,2,3,4,5\}$.

Simulation and Mesh Parameters
General Parameters
$\epsilon = 0.1, \quad D^{(i)} = 1, \quad \mathrm{Pe} = \epsilon^{-1}, \quad \mathrm{Da}_{k_1} = \epsilon^{-1},$ $\mathrm{Da}_{k_2} = \epsilon^{0}, \quad \theta_{k_3} = \epsilon^{0}$
Pore-scale Fluid Flow and Mass Transport
$r_\epsilon^{(1)} = 0.0175, \quad r_\epsilon^{(2)} = 0.0125, \quad r_\epsilon^{(3)} = 0.0100, \quad r_\epsilon^{(4)} = 0.0150,$ $A_\epsilon = \epsilon^2, \quad \Phi_\epsilon = 8\mathbf{e}_x, \quad N_{elem} = 38554, \quad \max(\Delta x) = 0.0036, \quad \Delta t = 10^{-5}$
Homogenized Mass Transport
$\phi = 0.7554, \quad N_{elem} = 4006, \quad \max(\Delta x) = 0.0113, \quad \Delta t = 10^{-6}$
Unit-cell Fluid Flow and Closure Problems
$r^{(1)} = 0.175, \quad r^{(2)} = 0.125, \quad r^{(3)} = 0.100, \quad r^{(4)} = 0.150,$ $A = 1, \quad \Phi = 8\mathbf{e}_\xi, \quad N_{elem} = 50856, \quad \max(\Delta \xi) = 0.0099$

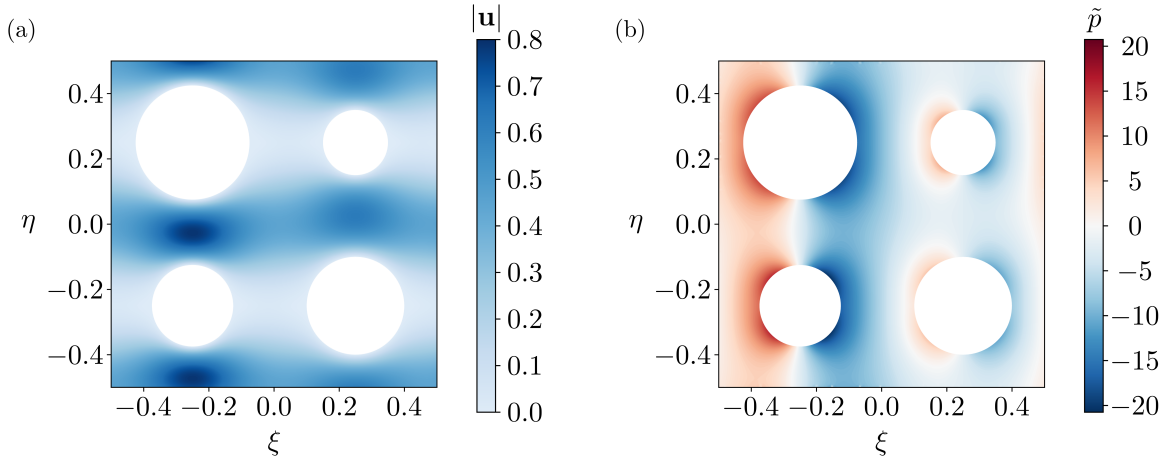

Figure 4. (a) The magnitude of the resulting flow velocity in the unit-cell. (b) The local pressure of the resulting flow in the unit-cell.

4.2.3 Pore-scale and Homogenized Model Results

With solutions to the flow and closure problems, the pore-scale (system (12)) and homogenized (system (15)) models are solved. Similar to before, the pore-scale solutions $c_\epsilon^{(i)}$, for $i \in \{1,2,3,4\}$, are averaged using the averaging operator in equation (22a*) to obtain the averaged pore-scale solutions $\langle c_\epsilon^{(i)} \rangle_{\mathcal{W}_\epsilon(\mathbf{x})}$. The absolute errors between $\langle c_\epsilon^{(i)} \rangle_{\mathcal{W}_\epsilon(\mathbf{x})}$ and the respective homogenized solutions $\langle c^{(i)} \rangle_Y$ are then calculated using equation (24*).

As shown in Figure 5, the averaged pore-scale and homogenized concentration profiles are plotted with their absolute errors. The qualitative comparisons in Figures 5(a), 5(c), 5(e), and 5(g) show matching profiles between the averaged pore-scale and homogenized solutions along the x-direction at all considered times. As time progresses, the initially discontinuous profiles become more uniform due to the diffusive and reactive dynamics of the system. Similar to before, the results are independent of y due to the periodicity of the problem.

Table 4. The simulation boundary conditions and initial conditions used to solve the various problems on the pore-scale, unit-cell, and continuum domains for the multi-species system undergoing linear and nonlinear, homogeneous and heterogeneous reactions. Here, $H(x)$ is the Heaviside function and $i \in \{1,2,3,4\}$. Also, $k_1 \in \{4\}$ and $k_2 \in \{1,2,3\}$ for $i \in \{1,3,4\}$, and $k_1 \in \{2\}$ and $k_2 \in \{1\}$ for $i \in \{2\}$.

Simulation Boundary Conditions

Pore-scale Mass Transport

$$c_\epsilon^{(i)}\Big|_{\partial\mathcal{B}_\epsilon^w} = c_\epsilon^{(i)}\Big|_{\partial\mathcal{B}_\epsilon^e} \qquad \mathbf{n}\cdot\nabla c_\epsilon^{(i)}\Big|_{\partial\mathcal{B}_\epsilon^w} = -\mathbf{n}\cdot\nabla c_\epsilon^{(i)}\Big|_{\partial\mathcal{B}_\epsilon^e}$$
$$c_\epsilon^{(i)}\Big|_{\partial\mathcal{B}_\epsilon^s} = c_\epsilon^{(i)}\Big|_{\partial\mathcal{B}_\epsilon^n} \qquad \mathbf{n}\cdot\nabla c_\epsilon^{(i)}\Big|_{\partial\mathcal{B}_\epsilon^s} = -\mathbf{n}\cdot\nabla c_\epsilon^{(i)}\Big|_{\partial\mathcal{B}_\epsilon^n}$$

Pore-scale Fluid Flow

$$\mathbf{u}_\epsilon|_{\partial\mathcal{B}_\epsilon^w} = \mathbf{u}_\epsilon|_{\partial\mathcal{B}_\epsilon^e} \qquad \mathbf{n}\cdot\nabla\mathbf{u}_\epsilon|_{\partial\mathcal{B}_\epsilon^w} = -\mathbf{n}\cdot\nabla\mathbf{u}_\epsilon|_{\partial\mathcal{B}_\epsilon^e}$$
$$\mathbf{u}_\epsilon|_{\partial\mathcal{B}_\epsilon^s} = \mathbf{u}_\epsilon|_{\partial\mathcal{B}_\epsilon^n} \qquad \mathbf{n}\cdot\nabla\mathbf{u}_\epsilon|_{\partial\mathcal{B}_\epsilon^s} = -\mathbf{n}\cdot\nabla\mathbf{u}_\epsilon|_{\partial\mathcal{B}_\epsilon^n}$$
$$\tilde{p}_\epsilon|_{\partial\mathcal{B}_\epsilon^w} = \tilde{p}_\epsilon|_{\partial\mathcal{B}_\epsilon^e} \qquad \mathbf{n}\cdot\nabla\tilde{p}_\epsilon|_{\partial\mathcal{B}_\epsilon^w} = -\mathbf{n}\cdot\nabla\tilde{p}_\epsilon|_{\partial\mathcal{B}_\epsilon^e}$$
$$\tilde{p}_\epsilon|_{\partial\mathcal{B}_\epsilon^s} = \tilde{p}_\epsilon|_{\partial\mathcal{B}_\epsilon^n} \qquad \mathbf{n}\cdot\nabla\tilde{p}_\epsilon|_{\partial\mathcal{B}_\epsilon^s} = -\mathbf{n}\cdot\nabla\tilde{p}_\epsilon|_{\partial\mathcal{B}_\epsilon^n}$$

Homogenized Mass Transport

$$\langle c^{(i)}\rangle_Y\Big|_{\partial\Omega^w} = \langle c^{(i)}\rangle_Y\Big|_{\partial\Omega^e} \qquad \mathbf{n}\cdot\nabla_{\mathbf{x}}\langle c^{(i)}\rangle_Y\Big|_{\partial\Omega^w} = -\mathbf{n}\cdot\nabla_{\mathbf{x}}\langle c^{(i)}\rangle_Y\Big|_{\partial\Omega^e}$$
$$\langle c^{(i)}\rangle_Y\Big|_{\partial\Omega^s} = \langle c^{(i)}\rangle_Y\Big|_{\partial\Omega^n} \qquad \mathbf{n}\cdot\nabla_{\mathbf{x}}\langle c^{(i)}\rangle_Y\Big|_{\partial\Omega^s} = -\mathbf{n}\cdot\nabla_{\mathbf{x}}\langle c^{(i)}\rangle_Y\Big|_{\partial\Omega^n}$$

Closure Problems

$$\boldsymbol{\chi}^{(i)[k_1]}\Big|_{\partial\mathcal{B}^w} = \boldsymbol{\chi}^{(i)[k_1]}\Big|_{\partial\mathcal{B}^e} \qquad \mathbf{n}\cdot\nabla_{\boldsymbol{\xi}}\boldsymbol{\chi}^{(i)[k_1]}\Big|_{\partial\mathcal{B}^w} = -\mathbf{n}\cdot\nabla_{\boldsymbol{\xi}}\boldsymbol{\chi}^{(i)[k_1]}\Big|_{\partial\mathcal{B}^e}$$
$$\boldsymbol{\chi}^{(i)[k_1]}\Big|_{\partial\mathcal{B}^s} = \boldsymbol{\chi}^{(i)[k_1]}\Big|_{\partial\mathcal{B}^n} \qquad \mathbf{n}\cdot\nabla_{\boldsymbol{\xi}}\boldsymbol{\chi}^{(i)[k_1]}\Big|_{\partial\mathcal{B}^s} = -\mathbf{n}\cdot\nabla_{\boldsymbol{\xi}}\boldsymbol{\chi}^{(i)[k_1]}\Big|_{\partial\mathcal{B}^n}$$
$$\chi^{(i)[k_2]}\Big|_{\partial\mathcal{B}^w} = \chi^{(i)[k_2]}\Big|_{\partial\mathcal{B}^e} \qquad \mathbf{n}\cdot\nabla_{\boldsymbol{\xi}}\chi^{(i)[k_2]}\Big|_{\partial\mathcal{B}^w} = -\mathbf{n}\cdot\nabla_{\boldsymbol{\xi}}\chi^{(i)[k_2]}\Big|_{\partial\mathcal{B}^e}$$
$$\chi^{(i)[k_2]}\Big|_{\partial\mathcal{B}^s} = \chi^{(i)[k_2]}\Big|_{\partial\mathcal{B}^n} \qquad \mathbf{n}\cdot\nabla_{\boldsymbol{\xi}}\chi^{(i)[k_2]}\Big|_{\partial\mathcal{B}^s} = -\mathbf{n}\cdot\nabla_{\boldsymbol{\xi}}\chi^{(i)[k_2]}\Big|_{\partial\mathcal{B}^n}$$

Unit-cell Fluid Flow

$$\mathbf{u}|_{\partial\mathcal{B}^w} = \mathbf{u}|_{\partial\mathcal{B}^e} \qquad \mathbf{n}\cdot\nabla_{\boldsymbol{\xi}}\mathbf{u}|_{\partial\mathcal{B}^w} = -\mathbf{n}\cdot\nabla_{\boldsymbol{\xi}}\mathbf{u}|_{\partial\mathcal{B}^e}$$
$$\mathbf{u}|_{\partial\mathcal{B}^s} = \mathbf{u}|_{\partial\mathcal{B}^n} \qquad \mathbf{n}\cdot\nabla_{\boldsymbol{\xi}}\mathbf{u}|_{\partial\mathcal{B}^s} = -\mathbf{n}\cdot\nabla_{\boldsymbol{\xi}}\mathbf{u}|_{\partial\mathcal{B}^n}$$
$$\tilde{p}|_{\partial\mathcal{B}^w} = \tilde{p}|_{\partial\mathcal{B}^e} \qquad \mathbf{n}\cdot\nabla_{\boldsymbol{\xi}}\tilde{p}|_{\partial\mathcal{B}^w} = -\mathbf{n}\cdot\nabla_{\boldsymbol{\xi}}\tilde{p}|_{\partial\mathcal{B}^e}$$
$$\tilde{p}|_{\partial\mathcal{B}^s} = \tilde{p}|_{\partial\mathcal{B}^n} \qquad \mathbf{n}\cdot\nabla_{\boldsymbol{\xi}}\tilde{p}|_{\partial\mathcal{B}^s} = -\mathbf{n}\cdot\nabla_{\boldsymbol{\xi}}\tilde{p}|_{\partial\mathcal{B}^n}$$

Simulation Initial Conditions

Pore-scale Mass Transport

$$c_\epsilon^{(1)} = 0.3H\,(-x) \quad \text{for} \quad (x,y) \in \mathcal{B}_\epsilon,\ t = 0$$
$$c_\epsilon^{(2)} = H\,(-x-0.25) \quad \text{for} \quad (x,y) \in \mathcal{B}_\epsilon,\ t = 0$$
$$c_\epsilon^{(3)} = 0.8H\,(x-0.15) \quad \text{for} \quad (x,y) \in \mathcal{B}_\epsilon,\ t = 0$$
$$c_\epsilon^{(4)} = 0.1H\,(x-0.25) \quad \text{for} \quad (x,y) \in \mathcal{B}_\epsilon,\ t = 0$$

Homogenized Mass Transport

$$\langle c^{(i)}\rangle_Y = \langle c_\epsilon^{(i)}\rangle_{\mathcal{W}_\epsilon(\mathbf{x})} \quad \text{for} \quad (x,y) \in \Omega,\ t = 0$$

In the quantitative comparisons shown in Figures 5(b), 5(d), 5(f), and 5(h), equation (24*) is used to calculate the absolute errors between the averaged pore-scale and homogenized concentration profiles along the x-direction at the considered times. As shown, the absolute errors remain below the error limit denoted by the red dotted lines for all considered times. Therefore, we deem the models valid and gain further confidence in the generalized closure form strategy encoded in Symbolica.

With the homogenized model validated, we reemphasize that Symbolica carried out the analytically intractable upscaling procedure required to homogenize the complex reaction network defined in system (10) in only 11 minutes with no human interaction. During this process, Symbolica defined nontrivial closure forms (system (14)) and formulated 14 unique closure problems using the encoded algorithm for the generalized closure form strategy with no prior knowledge about the closure of the system. We believe these abilities are invaluable for deploying Symbolica in subsurface engineering applications with realistic complexities.

5 Conclusion

In Part 2 of this series, we detailed an algorithmic procedure for applying the generalized closure form strategy and encoded it into our automated upscaling framework, Symbolica. We then validated its implementation by upscaling two reactive transport systems exhibiting moderately reactive physics, where diffusion and reaction terms are of the same order. In the first system, a solute undergoing a nonlinear heterogeneous reaction was considered. Using the encoded algorithm, Symbolica assumed an appropriate closure form at the first order, formulated valid closure problems, and ultimately derived a nonlinear homogenized model for the system, where the effective velocity and the effective reaction rate depended on the averaged concentration. Upon numerically validating this model, we emphasized the value of our encoded algorithm for upscaling realistic subsurface systems, where a broad range of complexities require nontrivial closure forms and closure problems to be defined.

In the second problem, we considered a complex multi-component system undergoing linear and nonlinear, homogeneous and heterogeneous reactions. Nontrivial closure forms and multiple closure problems were derived by Symbolica with no previous knowledge about the closure of the system. Similar to the previous problem, nonlinear effective parameters were found, including those of the emergent terms that appeared due to the bimolecular heterogeneous reactions. Upon numerically validating the models, our encoding of the generalized closure form strategy in Symbolica was further justified, and the benefits of automated closure form and closure problem definition for complex systems were again emphasized.

In summary, the work from this series 1) proposed and validated a strategy for extending the applicability of classical homogenization theory by generalizing closure forms, 2) developed an algorithm for implementing the strategy through automated upscaling frameworks like Symbolica, and 3) demonstrated the benefits of the encoded strategy. By demonstrating the capabilities and level of generalization automated upscaling frameworks can achieve, we hope to spark further interest in utilizing automated analytical frameworks for multi-scale modeling. Ultimately, this will facilitate a broader adoption and democratization of rigorous modeling techniques for geochemical reactive systems of realistic complexities (e.g., in CO_2 sequestration and H_2 storage), and create opportunities for method advancement using the paradigm of symbolic computation.

Acknowledgments

Support by the Department of Energy under the Early Career award DE-SC0019075 'Multiscale dynamics of reactive fronts in the subsurface' is gratefully acknowledged. KP was also supported by the Stanford Graduate Fellowship in Science and Engineering.

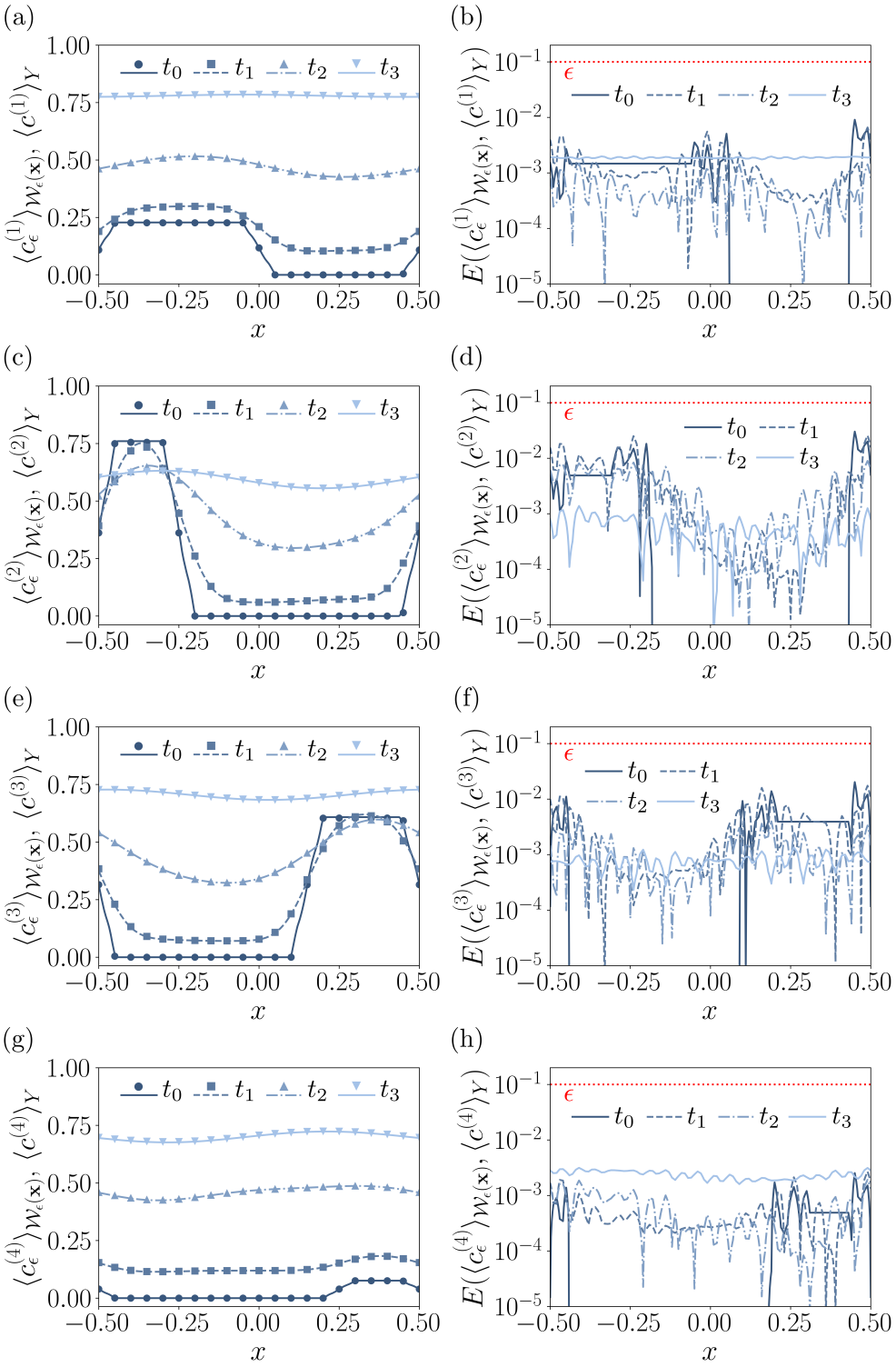

Figure 5. The numerical results for the system involving multiple species undergoing linear and nonlinear, homogeneous and heterogeneous reactions. The $\mathcal{W}_\epsilon(\mathbf{x})$-averaged and Y-averaged concentration profiles from the pore-scale (symbols) and homogenized (lines) models, respectively, are plotted for (a) $i = 1$, (c) $i = 2$, (e) $i = 3$, and (g) $i = 4$ at various times along the x-direction. The absolute errors between the averaged concentration profiles of $\langle c_\epsilon^{(i)}\rangle_{\mathcal{W}_\epsilon(\mathbf{x})}$ and $\langle c^{(i)}\rangle_Y$ are also plotted for (b) $i = 1$, (d) $i = 2$, (f) $i = 3$, and (h) $i = 4$ at various times along the x-direction. The upper error limit predicted by the homogenized model is displayed by the red dotted line. Here, $t_0 = 0$, $t_1 = 0.25 \times 10^{-2}$, $t_2 = 1.25 \times 10^{-2}$, and $t_3 = 3.75 \times 10^{-2}$.

Appendix A The Effective Parameters for the Nonlinear Homogeneous and Heterogeneous Reactions: Multiple Species

In this Appendix, we provide the effective parameters for system (15) derived by Symbolica in the problem considering a multi-species system undergoing linear and nonlinear, homogeneous and heterogeneous reactions with multiple reactive interfaces.

A1 Effective Parameters for Equation (15a)

$$\begin{aligned}\mathbf{U}^{(1)}\left(\langle c^{(3)}\rangle_Y\right) = \phi\mathrm{Pe}\langle\mathbf{u}\rangle_Y + \phi^2\frac{\mathrm{Da}_4}{|\mathcal{B}|}\left[|\Gamma^{(1)}|\langle\boldsymbol{\chi}^{(1)[4]}\rangle_{\Gamma^{(1)}} + |\Gamma^{(2)}|\langle\boldsymbol{\chi}^{(1)[4]}\rangle_{\Gamma^{(2)}} + |\Gamma^{(4)}|\langle\boldsymbol{\chi}^{(1)[4]}\rangle_{\Gamma^{(4)}}\right]\\ -\phi D^{(1)}\langle\nabla_{\boldsymbol{\xi}}\chi^{(1)[2]}\rangle_Y + \phi\mathrm{Pe}\epsilon\langle\mathbf{u}\chi^{(1)[2]}\rangle_Y\\ +\langle c^{(3)}\rangle_Y\left[\phi\frac{\mathrm{Da}_5}{|\mathcal{B}|}|\Gamma^{(1)}|\langle\boldsymbol{\chi}^{(1)[4]}\rangle_{\Gamma^{(1)}} - D^{(1)}\langle\nabla_{\boldsymbol{\xi}}\chi^{(1)[3]}\rangle_Y + \mathrm{Pe}\epsilon\langle\mathbf{u}\chi^{(1)[3]}\rangle_Y\right],\end{aligned} \tag{A1a}$$

$$\mathbf{V}^{(1)}\left(\langle c^{(1)}\rangle_Y\right) = \langle c^{(1)}\rangle_Y\left[\phi\frac{\mathrm{Da}_5}{|\mathcal{B}|}|\Gamma^{(1)}|\langle\boldsymbol{\chi}^{(3)[4]}\rangle_{\Gamma^{(1)}} - D^{(1)}\langle\nabla_{\boldsymbol{\xi}}\chi^{(1)[3]}\rangle_Y + \mathrm{Pe}\epsilon\langle\mathbf{u}\chi^{(1)[3]}\rangle_Y\right], \tag{A1b}$$

$$\mathbf{D}^{(1)} = \phi D^{(1)}\mathbf{I} + D^{(1)}\langle\nabla_{\boldsymbol{\xi}}\boldsymbol{\chi}^{(1)[4]}\rangle_Y - \mathrm{Pe}\epsilon\langle\mathbf{u}\otimes\boldsymbol{\chi}^{(1)[4]}\rangle_Y, \tag{A1c}$$

$$\begin{aligned}\mathscr{R}^{(1)}\left(\langle c^{(1)}\rangle_Y, \langle c^{(3)}\rangle_Y\right) = \mathscr{R}_1^{(1)}\left[\phi^2\langle c^{(1)}\rangle_Y - \phi^3\theta_1\right] + \mathscr{R}_2^{(1)}\left[\phi\langle c^{(1)}\rangle_Y\langle c^{(3)}\rangle_Y - \phi^3\theta_2\right]\\ +\phi^3\mathscr{R}_3^{(1)} + \phi^2\mathscr{R}_4^{(1)}\langle c^{(1)}\rangle_Y + \phi^2\mathscr{R}_5^{(1)}\langle c^{(3)}\rangle_Y + \phi\mathscr{R}_6^{(1)}\langle c^{(1)}\rangle_Y\langle c^{(3)}\rangle_Y\\ +\mathscr{R}_7^{(1)}\left[\langle c^{(1)}\rangle_Y\right]^2\langle c^{(3)}\rangle_Y + \mathscr{R}_8^{(1)}\langle c^{(1)}\rangle_Y\left[\langle c^{(3)}\rangle_Y\right]^2,\end{aligned} \tag{A1d}$$

A2 Effective Parameters for Equation (15b)

$$\begin{aligned}\mathbf{U}^{(2)}\left(\langle c^{(4)}\rangle_Y\right) = \phi\mathrm{Pe}\langle\mathbf{u}\rangle_Y + \langle c^{(4)}\rangle_Y\left[\phi\frac{\mathrm{Da}_8}{|\mathcal{B}|}\left(|\Gamma^{(2)}|\langle\boldsymbol{\chi}^{(2)[2]}\rangle_{\Gamma^{(2)}} + |\Gamma^{(3)}|\langle\boldsymbol{\chi}^{(2)[2]}\rangle_{\Gamma^{(3)}}\right.\right.\\ \left.\left.+|\Gamma^{(4)}|\langle\boldsymbol{\chi}^{(2)[2]}\rangle_{\Gamma^{(4)}}\right) - D^{(2)}\langle\nabla_{\boldsymbol{\xi}}\chi^{(2)[1]}\rangle_Y + \mathrm{Pe}\epsilon\langle\mathbf{u}\chi^{(2)[1]}\rangle_Y\right],\end{aligned} \tag{A2a}$$

$$\begin{aligned}\mathbf{V}^{(2)}\left(\langle c^{(2)}\rangle_Y\right) = \langle c^{(2)}\rangle_Y\left[\phi\frac{\mathrm{Da}_8}{|\mathcal{B}|}\left(|\Gamma^{(2)}|\langle\boldsymbol{\chi}^{(4)[4]}\rangle_{\Gamma^{(2)}} + |\Gamma^{(3)}|\langle\boldsymbol{\chi}^{(4)[4]}\rangle_{\Gamma^{(3)}} + |\Gamma^{(4)}|\langle\boldsymbol{\chi}^{(4)[4]}\rangle_{\Gamma^{(4)}}\right)\right.\\ \left.-D^{(2)}\langle\nabla_{\boldsymbol{\xi}}\chi^{(2)[1]}\rangle_Y + \mathrm{Pe}\epsilon\langle\mathbf{u}\chi^{(2)[1]}\rangle_Y\right],\end{aligned} \tag{A2b}$$

$$\mathbf{D}^{(2)} = \phi D^{(2)}\mathbf{I} + D^{(2)}\langle\nabla_{\boldsymbol{\xi}}\boldsymbol{\chi}^{(2)[2]}\rangle_Y - \mathrm{Pe}\epsilon\langle\mathbf{u}\otimes\boldsymbol{\chi}^{(2)[2]}\rangle_Y, \tag{A2c}$$

$$\begin{aligned}\mathscr{R}^{(2)}\left(\langle c^{(2)}\rangle_Y, \langle c^{(4)}\rangle_Y\right) = \mathscr{R}_1^{(2)}\left(\langle c^{(4)}\rangle_Y\right)\left[\langle c^{(2)}\rangle_Y\langle c^{(4)}\rangle_Y - \phi^2\theta_5\right] + \phi^2\mathscr{R}_2^{(2)}\langle c^{(2)}\rangle_Y\\ +\phi\mathscr{R}_3^{(2)}\langle c^{(2)}\rangle_Y\langle c^{(4)}\rangle_Y + \mathscr{R}_4^{(2)}\left[\langle c^{(2)}\rangle_Y\right]^2\langle c^{(4)}\rangle_Y.\end{aligned} \tag{A2d}$$

A3 Effective Parameters for Equation (15c)

$$\begin{aligned}\mathbf{U}^{(3)}\left(\langle c^{(1)}\rangle_Y\right) = \phi\mathrm{Pe}\langle\mathbf{u}\rangle_Y + \phi^2\frac{\mathrm{Da}_6}{|\mathcal{B}|}\left[|\Gamma^{(1)}|\langle\boldsymbol{\chi}^{(3)[4]}\rangle_{\Gamma^{(1)}} + |\Gamma^{(2)}|\langle\boldsymbol{\chi}^{(3)[4]}\rangle_{\Gamma^{(2)}}\right]\\ -\phi D^{(3)}\langle\nabla_{\boldsymbol{\xi}}\chi^{(3)[2]}\rangle_Y + \phi\mathrm{Pe}\epsilon\langle\mathbf{u}\chi^{(3)[2]}\rangle_Y\\ +\langle c^{(1)}\rangle_Y\left[\phi\frac{\mathrm{Da}_5}{|\mathcal{B}|}|\Gamma^{(1)}|\langle\boldsymbol{\chi}^{(3)[4]}\rangle_{\Gamma^{(1)}} - D^{(3)}\langle\nabla_{\boldsymbol{\xi}}\chi^{(3)[3]}\rangle_Y + \mathrm{Pe}\epsilon\langle\mathbf{u}\chi^{(3)[3]}\rangle_Y\right],\end{aligned} \tag{A3a}$$

$$\mathbf{V}^{(3)}\left(\langle c^{(3)}\rangle_Y\right) = \langle c^{(3)}\rangle_Y\left[\phi\frac{\mathrm{Da}_5}{|\mathcal{B}|}|\Gamma^{(1)}|\langle\boldsymbol{\chi}^{(1)[4]}\rangle_{\Gamma^{(1)}} - D^{(3)}\langle\nabla_{\boldsymbol{\xi}}\chi^{(3)[3]}\rangle_Y + \mathrm{Pe}\epsilon\langle\mathbf{u}\chi^{(3)[3]}\rangle_Y\right], \tag{A3b}$$

$$\mathbf{D}^{(3)} = \phi D^{(3)}\mathbf{I} + D^{(3)}\langle\nabla_{\boldsymbol{\xi}}\boldsymbol{\chi}^{(3)[4]}\rangle_Y - \mathrm{Pe}\epsilon\langle\mathbf{u}\otimes\boldsymbol{\chi}^{(3)[4]}\rangle_Y, \tag{A3c}$$

$$\begin{aligned}\mathscr{R}^{(3)}\left(\langle c^{(1)}\rangle_Y, \langle c^{(3)}\rangle_Y\right) &= \mathscr{R}_1^{(3)}\left[\phi^2\langle c^{(3)}\rangle_Y - \phi^3\theta_3\right] + \mathscr{R}_2^{(3)}\left[\phi\langle c^{(1)}\rangle_Y\langle c^{(3)}\rangle_Y - \phi^3\theta_2\right]\\ &+\phi^3\mathscr{R}_3^{(3)} + \phi^2\mathscr{R}_4^{(3)}\langle c^{(1)}\rangle_Y + \phi^2\mathscr{R}_5^{(3)}\langle c^{(3)}\rangle_Y + \phi\mathscr{R}_6^{(3)}\langle c^{(1)}\rangle_Y\langle c^{(3)}\rangle_Y + \mathscr{R}_7^{(3)}\left[\langle c^{(1)}\rangle_Y\right]^2\langle c^{(3)}\rangle_Y\\ &+\mathscr{R}_8^{(3)}\langle c^{(1)}\rangle_Y\left[\langle c^{(3)}\rangle_Y\right]^2.\end{aligned} \tag{A3d}$$

A4 Effective Parameters for Equation (15d)

$$\begin{aligned}\mathbf{U}^{(4)}\left(\langle c^{(2)}\rangle_Y\right) &= \phi\mathrm{Pe}\langle\mathbf{u}\rangle_Y + \phi^2\frac{\mathrm{Da}_7}{|\mathcal{B}|}\left[|\Gamma^{(1)}|\langle\boldsymbol{\chi}^{(4)[4]}\rangle_{\Gamma^{(1)}} + |\Gamma^{(3)}|\langle\boldsymbol{\chi}^{(4)[4]}\rangle_{\Gamma^{(3)}} + |\Gamma^{(4)}|\langle\boldsymbol{\chi}^{(4)[4]}\rangle_{\Gamma^{(4)}}\right]\\ &-\phi D^{(4)}\langle\nabla_{\boldsymbol{\xi}}\chi^{(4)[2]}\rangle_Y + \phi\mathrm{Pe}\epsilon\langle\mathbf{u}\chi^{(4)[2]}\rangle_Y\\ &+\langle c^{(2)}\rangle_Y\left[\phi\frac{\mathrm{Da}_8}{|\mathcal{B}|}\left(|\Gamma^{(2)}|\langle\boldsymbol{\chi}^{(4)[4]}\rangle_{\Gamma^{(2)}} + |\Gamma^{(3)}|\langle\boldsymbol{\chi}^{(4)[4]}\rangle_{\Gamma^{(3)}}\right.\right.\\ &\left.\left.+|\Gamma^{(4)}|\langle\boldsymbol{\chi}^{(4)[4]}\rangle_{\Gamma^{(4)}}\right) - D^{(4)}\langle\nabla_{\boldsymbol{\xi}}\chi^{(4)[3]}\rangle_Y + \mathrm{Pe}\epsilon\langle\mathbf{u}\chi^{(4)[3]}\rangle_Y\right],\end{aligned} \tag{A4a}$$

$$\begin{aligned}\mathbf{V}^{(4)}\left(\langle c^{(4)}\rangle_Y\right) &= \langle c^{(4)}\rangle_Y\left[\phi\frac{\mathrm{Da}_8}{|\mathcal{B}|}\left(|\Gamma^{(2)}|\langle\boldsymbol{\chi}^{(2)[2]}\rangle_{\Gamma^{(2)}} + |\Gamma^{(3)}|\langle\boldsymbol{\chi}^{(2)[2]}\rangle_{\Gamma^{(3)}} + |\Gamma^{(4)}|\langle\boldsymbol{\chi}^{(2)[2]}\rangle_{\Gamma^{(4)}}\right)\right.\\ &\left.-D^{(4)}\langle\nabla_{\boldsymbol{\xi}}\chi^{(4)[3]}\rangle_Y + \mathrm{Pe}\epsilon\langle\mathbf{u}\chi^{(4)[3]}\rangle_Y\right],\end{aligned} \tag{A4b}$$

$$\mathbf{D}^{(4)} = \phi D^{(4)}\mathbf{I} + D^{(4)}\langle\nabla_{\boldsymbol{\xi}}\boldsymbol{\chi}^{(4)[4]}\rangle_Y - \mathrm{Pe}\epsilon\langle\mathbf{u}\otimes\boldsymbol{\chi}^{(4)[4]}\rangle_Y, \tag{A4c}$$

$$\begin{aligned}\mathscr{R}^{(4)}\left(\langle c^{(2)}\rangle_Y, \langle c^{(4)}\rangle_Y\right) &= \mathscr{R}_1^{(4)}\left[\phi^2\langle c^{(4)}\rangle_Y - \phi^3\theta_4\right] + \mathscr{R}_2^{(4)}\left(\langle c^{(4)}\rangle_Y\right)\left[\langle c^{(2)}\rangle_Y\langle c^{(4)}\rangle_Y - \phi^2\theta_5\right]\\ &+\phi^3\mathscr{R}_3^{(4)} + \phi^2\mathscr{R}_4^{(4)}\langle c^{(2)}\rangle_Y + \phi^2\mathscr{R}_5^{(4)}\langle c^{(4)}\rangle_Y + \phi\mathscr{R}_6^{(4)}\langle c^{(2)}\rangle_Y\langle c^{(4)}\rangle_Y + \mathscr{R}_7^{(4)}\left[\langle c^{(2)}\rangle_Y\right]^2\langle c^{(4)}\rangle_Y.\end{aligned} \tag{A4d}$$

Appendix B The Effective Reaction Sub-parameters for the Nonlinear Homogeneous and Heterogeneous Reactions: Multiple Species

In this Appendix, we provide the sub-parameters for the effective reaction rates derived by Symbolica in the problem considering a multi-species system undergoing linear and nonlinear, homogeneous and heterogeneous reactions with multiple reactive interfaces.

B1 Effective Reaction Sub-parameters for $\mathscr{R}^{(1)}\left(\langle \boldsymbol{c}^{(1)}\rangle_{\boldsymbol{Y}}, \langle \boldsymbol{c}^{(3)}\rangle_{\boldsymbol{Y}}\right)$

$$\mathscr{R}_1^{(1)} = \frac{\mathrm{Da}_4}{|\mathcal{B}|\,\epsilon}\left(|\Gamma^{(1)}| + |\Gamma^{(2)}| + |\Gamma^{(4)}|\right), \tag{B1a}$$

$$\mathscr{R}_2^{(1)} = \frac{\mathrm{Da}_5}{|\mathcal{B}|\,\epsilon}|\Gamma^{(1)}|, \tag{B1b}$$

$$\mathscr{R}_3^{(1)} = \frac{\mathrm{Da}_4}{|\mathcal{B}|}\left(|\Gamma^{(1)}|\langle\chi^{(1)[1]}\rangle_{\Gamma^{(1)}} + |\Gamma^{(2)}|\langle\chi^{(1)[1]}\rangle_{\Gamma^{(2)}} + |\Gamma^{(4)}|\langle\chi^{(1)[1]}\rangle_{\Gamma^{(4)}}\right), \tag{B1c}$$

$$\begin{aligned}\mathscr{R}_4^{(1)} = \frac{\mathrm{Da}_4}{|\mathcal{B}|}&\left(|\Gamma^{(1)}|\langle\chi^{(1)[2]}\rangle_{\Gamma^{(1)}} + |\Gamma^{(2)}|\langle\chi^{(1)[2]}\rangle_{\Gamma^{(2)}} + |\Gamma^{(4)}|\langle\chi^{(1)[2]}\rangle_{\Gamma^{(4)}}\right)\\ &+\frac{\mathrm{Da}_5}{|\mathcal{B}|}|\Gamma^{(1)}|\langle\chi^{(3)[1]}\rangle_{\Gamma^{(1)}},\end{aligned} \tag{B1d}$$

$$\mathscr{R}_5^{(1)} = \frac{\mathrm{Da}_5}{|\mathcal{B}|}|\Gamma^{(1)}|\langle\chi^{(1)[1]}\rangle_{\Gamma^{(1)}}, \tag{B1e}$$

$$\begin{aligned}\mathscr{R}_6^{(1)} = \frac{\mathrm{Da}_4}{|\mathcal{B}|}&\left(|\Gamma^{(1)}|\langle\chi^{(1)[3]}\rangle_{\Gamma^{(1)}} + |\Gamma^{(2)}|\langle\chi^{(1)[3]}\rangle_{\Gamma^{(2)}} + |\Gamma^{(4)}|\langle\chi^{(1)[3]}\rangle_{\Gamma^{(4)}}\right)\\ &+\frac{\mathrm{Da}_5}{|\mathcal{B}|}\left(|\Gamma^{(1)}|\langle\chi^{(3)[2]}\rangle_{\Gamma^{(1)}} + |\Gamma^{(1)}|\langle\chi^{(1)[2]}\rangle_{\Gamma^{(1)}}\right),\end{aligned} \tag{B1f}$$

$$\mathscr{R}_7^{(1)} = \frac{\mathrm{Da}_5}{|\mathcal{B}|}|\Gamma^{(1)}|\langle\chi^{(3)[3]}\rangle_{\Gamma^{(1)}}, \tag{B1g}$$

$$\mathscr{R}_8^{(1)} = \frac{\mathrm{Da}_5}{|\mathcal{B}|}|\Gamma^{(1)}|\langle\chi^{(1)[3]}\rangle_{\Gamma^{(1)}}. \tag{B1h}$$

B2 Effective Reaction Sub-parameters for $\mathscr{R}^{(2)}\left(\langle \boldsymbol{c}^{(2)}\rangle_{\boldsymbol{Y}}, \langle \boldsymbol{c}^{(4)}\rangle_{\boldsymbol{Y}}\right)$

$$\begin{aligned}\mathscr{R}_1^{(2)}\left(\langle c^{(4)}\rangle_Y\right) = \frac{\mathrm{Da}_8}{|\mathcal{B}|}&\left[\phi\epsilon^{-1}\left(|\Gamma^{(2)}| + |\Gamma^{(3)}| + |\Gamma^{(4)}|\right)\right.\\ &\left.+\langle c^{(4)}\rangle_Y\left(|\Gamma^{(2)}|\langle\chi^{(2)[1]}\rangle_{\Gamma^{(2)}} + |\Gamma^{(3)}|\langle\chi^{(2)[1]}\rangle_{\Gamma^{(3)}} + |\Gamma^{(4)}|\langle\chi^{(2)[1]}\rangle_{\Gamma^{(4)}}\right)\right],\end{aligned} \tag{B2a}$$

$$\mathscr{R}_2^{(2)} = \frac{\mathrm{Da}_8}{|\mathcal{B}|}\left(|\Gamma^{(2)}|\langle\chi^{(4)[1]}\rangle_{\Gamma^{(2)}} + |\Gamma^{(3)}|\langle\chi^{(4)[1]}\rangle_{\Gamma^{(3)}} + |\Gamma^{(4)}|\langle\chi^{(4)[1]}\rangle_{\Gamma^{(4)}}\right), \tag{B2b}$$

$$\mathscr{R}_3^{(2)} = \frac{\mathrm{Da}_8}{|\mathcal{B}|}\left(|\Gamma^{(2)}|\langle\chi^{(4)[2]}\rangle_{\Gamma^{(2)}} + |\Gamma^{(3)}|\langle\chi^{(4)[2]}\rangle_{\Gamma^{(3)}} + |\Gamma^{(4)}|\langle\chi^{(4)[2]}\rangle_{\Gamma^{(4)}}\right), \tag{B2c}$$

$$\mathscr{R}_4^{(2)} = \frac{\mathrm{Da}_8}{|\mathcal{B}|}\left(|\Gamma^{(2)}|\langle\chi^{(4)[3]}\rangle_{\Gamma^{(2)}} + |\Gamma^{(3)}|\langle\chi^{(4)[3]}\rangle_{\Gamma^{(3)}} + |\Gamma^{(4)}|\langle\chi^{(4)[3]}\rangle_{\Gamma^{(4)}}\right). \tag{B2d}$$

B3 Effective Reaction Sub-parameters for $\mathscr{R}^{(3)}\left(\langle \boldsymbol{c^{(1)}}\rangle_{\boldsymbol{Y}}, \langle \boldsymbol{c^{(3)}}\rangle_{\boldsymbol{Y}}\right)$

$$\mathscr{R}_1^{(3)} = \frac{\mathrm{Da}_6}{|\mathcal{B}|\,\epsilon}\left(|\Gamma^{(1)}| + |\Gamma^{(2)}|\right), \tag{B3a}$$

$$\mathscr{R}_2^{(3)} = \frac{\mathrm{Da}_5}{|\mathcal{B}|\,\epsilon}|\Gamma^{(1)}|, \tag{B3b}$$

$$\mathscr{R}_3^{(3)} = \frac{\mathrm{Da}_6}{|\mathcal{B}|}\left(|\Gamma^{(1)}|\langle\chi^{(3)[1]}\rangle_{\Gamma^{(1)}} + |\Gamma^{(2)}|\langle\chi^{(3)[1]}\rangle_{\Gamma^{(2)}}\right), \tag{B3c}$$

$$\mathscr{R}_4^{(3)} = \frac{\mathrm{Da}_5}{|\mathcal{B}|}|\Gamma^{(1)}|\langle\chi^{(3)[1]}\rangle_{\Gamma^{(1)}}, \tag{B3d}$$

$$\mathscr{R}_5^{(3)} = \frac{\mathrm{Da}_5}{|\mathcal{B}|}|\Gamma^{(1)}|\langle\chi^{(1)[1]}\rangle_{\Gamma^{(1)}} + \frac{\mathrm{Da}_6}{|\mathcal{B}|}\left(|\Gamma^{(1)}|\langle\chi^{(3)[2]}\rangle_{\Gamma^{(1)}} + |\Gamma^{(2)}|\langle\chi^{(3)[2]}\rangle_{\Gamma^{(2)}}\right), \tag{B3e}$$

$$\begin{aligned}\mathscr{R}_6^{(3)} = \frac{\mathrm{Da}_5}{|\mathcal{B}|}\left(|\Gamma^{(1)}|\langle\chi^{(1)[2]}\rangle_{\Gamma^{(1)}} + |\Gamma^{(1)}|\langle\chi^{(3)[2]}\rangle_{\Gamma^{(1)}}\right)\\ +\frac{\mathrm{Da}_6}{|\mathcal{B}|}\left(|\Gamma^{(1)}|\langle\chi^{(3)[3]}\rangle_{\Gamma^{(1)}} + |\Gamma^{(2)}|\langle\chi^{(3)[3]}\rangle_{\Gamma^{(2)}}\right),\end{aligned} \tag{B3f}$$

$$\mathscr{R}_7^{(3)} = \frac{\mathrm{Da}_5}{|\mathcal{B}|}|\Gamma^{(1)}|\langle\chi^{(3)[3]}\rangle_{\Gamma^{(1)}}, \tag{B3g}$$

$$\mathscr{R}_8^{(3)} = \frac{\mathrm{Da}_5}{|\mathcal{B}|}|\Gamma^{(1)}|\langle\chi^{(1)[3]}\rangle_{\Gamma^{(1)}}. \tag{B3h}$$

B4 Effective Reaction Sub-parameters for $\mathscr{R}^{(4)}\left(\langle \boldsymbol{c^{(2)}}\rangle_{\boldsymbol{Y}}, \langle \boldsymbol{c^{(4)}}\rangle_{\boldsymbol{Y}}\right)$

$$\mathscr{R}_1^{(4)} = \frac{\mathrm{Da}_7}{|\mathcal{B}|\,\epsilon}\left(|\Gamma^{(1)}| + |\Gamma^{(3)}| + |\Gamma^{(4)}|\right), \tag{B4a}$$

$$\begin{aligned}\mathscr{R}_2^{(4)}\left(\langle c^{(4)}\rangle_Y\right) = \frac{\mathrm{Da}_8}{|\mathcal{B}|}\left[\phi\epsilon^{-1}\left(|\Gamma^{(2)}| + |\Gamma^{(3)}| + |\Gamma^{(4)}|\right)\right.\\ \left.+\langle c^{(4)}\rangle_Y\left(|\Gamma^{(2)}|\langle\chi^{(2)[1]}\rangle_{\Gamma^{(2)}} + |\Gamma^{(3)}|\langle\chi^{(2)[1]}\rangle_{\Gamma^{(3)}} + |\Gamma^{(4)}|\langle\chi^{(2)[1]}\rangle_{\Gamma^{(4)}}\right)\right],\end{aligned} \tag{B4b}$$

$$\mathscr{R}_3^{(4)} = \frac{\mathrm{Da}_7}{|\mathcal{B}|}\left(|\Gamma^{(1)}|\langle\chi^{(4)[1]}\rangle_{\Gamma^{(1)}} + |\Gamma^{(3)}|\langle\chi^{(4)[1]}\rangle_{\Gamma^{(3)}} + |\Gamma^{(4)}|\langle\chi^{(4)[1]}\rangle_{\Gamma^{(4)}}\right), \tag{B4c}$$

$$\mathscr{R}_4^{(4)} = \frac{\mathrm{Da}_8}{|\mathcal{B}|}\left(|\Gamma^{(2)}|\langle\chi^{(4)[1]}\rangle_{\Gamma^{(2)}} + |\Gamma^{(3)}|\langle\chi^{(4)[1]}\rangle_{\Gamma^{(3)}} + |\Gamma^{(4)}|\langle\chi^{(4)[1]}\rangle_{\Gamma^{(4)}}\right), \tag{B4d}$$

$$\mathscr{R}_5^{(4)} = \frac{\mathrm{Da}_7}{|\mathcal{B}|}\left(|\Gamma^{(1)}|\langle\chi^{(4)[2]}\rangle_{\Gamma^{(1)}} + |\Gamma^{(3)}|\langle\chi^{(4)[2]}\rangle_{\Gamma^{(3)}} + |\Gamma^{(4)}|\langle\chi^{(4)[2]}\rangle_{\Gamma^{(4)}}\right), \tag{B4e}$$

$$\begin{aligned}\mathscr{R}_6^{(4)} = \frac{\mathrm{Da}_7}{|\mathcal{B}|}\left(|\Gamma^{(1)}|\langle\chi^{(4)[3]}\rangle_{\Gamma^{(1)}} + |\Gamma^{(3)}|\langle\chi^{(4)[3]}\rangle_{\Gamma^{(3)}} + |\Gamma^{(4)}|\langle\chi^{(4)[3]}\rangle_{\Gamma^{(4)}}\right)\\ +\frac{\mathrm{Da}_8}{|\mathcal{B}|}\left(|\Gamma^{(2)}|\langle\chi^{(4)[2]}\rangle_{\Gamma^{(2)}} + |\Gamma^{(3)}|\langle\chi^{(4)[2]}\rangle_{\Gamma^{(3)}} + |\Gamma^{(4)}|\langle\chi^{(4)[2]}\rangle_{\Gamma^{(4)}}\right),\end{aligned} \tag{B4f}$$

$$\mathscr{R}_7^{(4)} = \frac{\mathrm{Da}_8}{|\mathcal{B}|}\left(|\Gamma^{(2)}|\langle\chi^{(4)[3]}\rangle_{\Gamma^{(2)}} + |\Gamma^{(3)}|\langle\chi^{(4)[3]}\rangle_{\Gamma^{(3)}} + |\Gamma^{(4)}|\langle\chi^{(4)[3]}\rangle_{\Gamma^{(4)}}\right). \tag{B4g}$$

Appendix C The Closure Problems for the Nonlinear Homogeneous and Heterogeneous Reactions: Multiple Species

In this Appendix, we provide the closure problems derived by Symbolica for the problem considering a multi-species system undergoing linear and nonlinear, homogeneous and heterogeneous reactions with multiple reactive interfaces.

C1 Closure Problems for $c_1^{(1)}$:

C11 Closure Problem for $\chi^{(1)[1]}$

$$\begin{aligned}\frac{\mathrm{Da}_4\theta_1}{|\mathcal{B}|}\left(|\Gamma^{(1)}|+|\Gamma^{(2)}|+|\Gamma^{(4)}|\right)+\frac{\mathrm{Da}_5\theta_2}{|\mathcal{B}|}|\Gamma^{(1)}|\\ +\mathrm{Pe}\epsilon\mathbf{u}_0\cdot\nabla_{\boldsymbol{\xi}}\chi^{(1)[1]}-D^{(1)}\nabla^2_{\boldsymbol{\xi}}\chi^{(1)[1]}=0\quad\text{for }\boldsymbol{\xi}\in\mathcal{B},\end{aligned}\tag{C1a}$$

$$-\mathbf{n}^{(1)}\cdot D^{(1)}\nabla_{\boldsymbol{\xi}}\chi^{(1)[1]}=-\mathrm{Da}_4\theta_1-\mathrm{Da}_5\theta_2\quad\text{for }\boldsymbol{\xi}\in\Gamma^{(1)},\tag{C1b}$$

$$-\mathbf{n}^{(2)}\cdot D^{(1)}\nabla_{\boldsymbol{\xi}}\chi^{(1)[1]}=-\mathrm{Da}_4\theta_1\quad\text{for }\boldsymbol{\xi}\in\Gamma^{(2)},\tag{C1c}$$

$$-\mathbf{n}^{(3)}\cdot D^{(1)}\nabla_{\boldsymbol{\xi}}\chi^{(1)[1]}=0\quad\text{for }\boldsymbol{\xi}\in\Gamma^{(3)},\tag{C1d}$$

$$-\mathbf{n}^{(4)}\cdot D^{(1)}\nabla_{\boldsymbol{\xi}}\chi^{(1)[1]}=-\mathrm{Da}_4\theta_1\quad\text{for }\boldsymbol{\xi}\in\Gamma^{(4)}.\tag{C1e}$$

C12 Closure Problem for $\chi^{(1)[2]}$

$$-\frac{\mathrm{Da}_4}{|\mathcal{B}|}\left(|\Gamma^{(1)}|+|\Gamma^{(2)}|+|\Gamma^{(4)}|\right)+\mathrm{Pe}\epsilon\mathbf{u}_0\cdot\nabla_{\boldsymbol{\xi}}\chi^{(1)[2]}-D^{(1)}\nabla^2_{\boldsymbol{\xi}}\chi^{(1)[2]}=0\quad\text{for }\boldsymbol{\xi}\in\mathcal{B},\tag{C2a}$$

$$-\mathbf{n}^{(1)}\cdot D^{(1)}\nabla_{\boldsymbol{\xi}}\chi^{(1)[2]}=\mathrm{Da}_4\quad\text{for }\boldsymbol{\xi}\in\Gamma^{(1)},\tag{C2b}$$

$$-\mathbf{n}^{(2)}\cdot D^{(1)}\nabla_{\boldsymbol{\xi}}\chi^{(1)[2]}=\mathrm{Da}_4\quad\text{for }\boldsymbol{\xi}\in\Gamma^{(2)},\tag{C2c}$$

$$-\mathbf{n}^{(3)}\cdot D^{(1)}\nabla_{\boldsymbol{\xi}}\chi^{(1)[2]}=0\quad\text{for }\boldsymbol{\xi}\in\Gamma^{(3)},\tag{C2d}$$

$$-\mathbf{n}^{(4)}\cdot D^{(1)}\nabla_{\boldsymbol{\xi}}\chi^{(1)[2]}=\mathrm{Da}_4\quad\text{for }\boldsymbol{\xi}\in\Gamma^{(4)}.\tag{C2e}$$

C13 Closure Problem for $\chi^{(1)[3]}$

$$-\frac{\mathrm{Da}_5}{|\mathcal{B}|}|\Gamma^{(1)}|+\mathrm{Pe}\epsilon\mathbf{u}_0\cdot\nabla_{\boldsymbol{\xi}}\chi^{(1)[3]}-D^{(1)}\nabla^2_{\boldsymbol{\xi}}\chi^{(1)[3]}=0\quad\text{for }\boldsymbol{\xi}\in\mathcal{B},\tag{C3a}$$

$$-\mathbf{n}^{(1)}\cdot D^{(1)}\nabla_{\boldsymbol{\xi}}\chi^{(1)[3]}=\mathrm{Da}_5\quad\text{for }\boldsymbol{\xi}\in\Gamma^{(1)},\tag{C3b}$$

$$-\mathbf{n}^{(2)}\cdot D^{(1)}\nabla_{\boldsymbol{\xi}}\chi^{(1)[3]}=0\quad\text{for }\boldsymbol{\xi}\in\Gamma^{(2)},\tag{C3c}$$

$$-\mathbf{n}^{(3)}\cdot D^{(1)}\nabla_{\boldsymbol{\xi}}\chi^{(1)[3]}=0\quad\text{for }\boldsymbol{\xi}\in\Gamma^{(3)},\tag{C3d}$$

$$-\mathbf{n}^{(4)}\cdot D^{(1)}\nabla_{\boldsymbol{\xi}}\chi^{(1)[3]}=0\quad\text{for }\boldsymbol{\xi}\in\Gamma^{(4)}.\tag{C3e}$$

C14 Closure Problem for $\boldsymbol{\chi^{(1)[4]}}$

$$\mathrm{Pe}\epsilon\left(\mathbf{u}_0 - \langle \mathbf{u}_0 \rangle_{\mathcal{B}}\right) + \mathrm{Pe}\epsilon \mathbf{u}_0 \cdot \nabla_{\boldsymbol{\xi}} \boldsymbol{\chi}^{(1)[4]} - D^{(1)} \nabla_{\boldsymbol{\xi}} \cdot \left(\mathbf{I} + \nabla_{\boldsymbol{\xi}} \boldsymbol{\chi}^{(1)[4]}\right) = \mathbf{0} \quad \text{for } \boldsymbol{\xi} \in \mathcal{B}, \tag{C4a}$$

$$-\mathbf{n}^{(1)} \cdot D^{(1)} \left(\mathbf{I} + \nabla_{\boldsymbol{\xi}} \boldsymbol{\chi}^{(1)[4]}\right) = \mathbf{0} \quad \text{for } \boldsymbol{\xi} \in \Gamma^{(1)}, \tag{C4b}$$

$$-\mathbf{n}^{(2)} \cdot D^{(1)} \left(\mathbf{I} + \nabla_{\boldsymbol{\xi}} \boldsymbol{\chi}^{(1)[4]}\right) = \mathbf{0} \quad \text{for } \boldsymbol{\xi} \in \Gamma^{(2)}, \tag{C4c}$$

$$-\mathbf{n}^{(3)} \cdot D^{(1)} \left(\mathbf{I} + \nabla_{\boldsymbol{\xi}} \boldsymbol{\chi}^{(1)[4]}\right) = \mathbf{0} \quad \text{for } \boldsymbol{\xi} \in \Gamma^{(3)}, \tag{C4d}$$

$$-\mathbf{n}^{(4)} \cdot D^{(1)} \left(\mathbf{I} + \nabla_{\boldsymbol{\xi}} \boldsymbol{\chi}^{(1)[4]}\right) = \mathbf{0} \quad \text{for } \boldsymbol{\xi} \in \Gamma^{(4)}. \tag{C4e}$$

C2 Closure Problems for $\boldsymbol{c_1^{(2)}}$:

C21 Closure Problem for $\boldsymbol{\chi^{(2)[1]}}$

$$-\frac{\mathrm{Da}_8}{|\mathcal{B}|}\left(|\Gamma^{(2)}| + |\Gamma^{(3)}| + |\Gamma^{(4)}|\right) + \mathrm{Pe}\epsilon \mathbf{u}_0 \cdot \nabla_{\boldsymbol{\xi}} \chi^{(2)[1]} - D^{(2)} \nabla^2_{\boldsymbol{\xi}} \chi^{(2)[1]} = 0 \quad \text{for } \boldsymbol{\xi} \in \mathcal{B}, \tag{C5a}$$

$$-\mathbf{n}^{(1)} \cdot D^{(2)} \nabla_{\boldsymbol{\xi}} \chi^{(2)[1]} = 0 \quad \text{for } \boldsymbol{\xi} \in \Gamma^{(1)}, \tag{C5b}$$

$$-\mathbf{n}^{(2)} \cdot D^{(2)} \nabla_{\boldsymbol{\xi}} \chi^{(2)[1]} = \mathrm{Da}_8 \quad \text{for } \boldsymbol{\xi} \in \Gamma^{(2)}, \tag{C5c}$$

$$-\mathbf{n}^{(3)} \cdot D^{(2)} \nabla_{\boldsymbol{\xi}} \chi^{(2)[1]} = \mathrm{Da}_8 \quad \text{for } \boldsymbol{\xi} \in \Gamma^{(3)}, \tag{C5d}$$

$$-\mathbf{n}^{(4)} \cdot D^{(2)} \nabla_{\boldsymbol{\xi}} \chi^{(2)[1]} = \mathrm{Da}_8 \quad \text{for } \boldsymbol{\xi} \in \Gamma^{(4)}. \tag{C5e}$$

C22 Closure Problem for $\boldsymbol{\chi^{(2)[2]}}$

$$\mathrm{Pe}\epsilon\left(\mathbf{u}_0 - \langle \mathbf{u}_0 \rangle_{\mathcal{B}}\right) + \mathrm{Pe}\epsilon \mathbf{u}_0 \cdot \nabla_{\boldsymbol{\xi}} \boldsymbol{\chi}^{(2)[2]} - D^{(2)} \nabla_{\boldsymbol{\xi}} \cdot \left(\mathbf{I} + \nabla_{\boldsymbol{\xi}} \boldsymbol{\chi}^{(2)[2]}\right) = \mathbf{0} \quad \text{for } \boldsymbol{\xi} \in \mathcal{B}, \tag{C6a}$$

$$-\mathbf{n}^{(1)} \cdot D^{(2)} \left(\mathbf{I} + \nabla_{\boldsymbol{\xi}} \boldsymbol{\chi}^{(2)[2]}\right) = \mathbf{0} \quad \text{for } \boldsymbol{\xi} \in \Gamma^{(1)}, \tag{C6b}$$

$$-\mathbf{n}^{(2)} \cdot D^{(2)} \left(\mathbf{I} + \nabla_{\boldsymbol{\xi}} \boldsymbol{\chi}^{(2)[2]}\right) = \mathbf{0} \quad \text{for } \boldsymbol{\xi} \in \Gamma^{(2)}, \tag{C6c}$$

$$-\mathbf{n}^{(3)} \cdot D^{(2)} \left(\mathbf{I} + \nabla_{\boldsymbol{\xi}} \boldsymbol{\chi}^{(2)[2]}\right) = \mathbf{0} \quad \text{for } \boldsymbol{\xi} \in \Gamma^{(3)}, \tag{C6d}$$

$$-\mathbf{n}^{(4)} \cdot D^{(2)} \left(\mathbf{I} + \nabla_{\boldsymbol{\xi}} \boldsymbol{\chi}^{(2)[2]}\right) = \mathbf{0} \quad \text{for } \boldsymbol{\xi} \in \Gamma^{(4)}. \tag{C6e}$$

C3 Closure Problems for $c_1^{(3)}$:

C31 Closure Problem for $\boldsymbol{\chi^{(3)[1]}}$

$$\frac{\mathrm{Da}_5\theta_2}{|\mathcal{B}|}|\Gamma^{(1)}| + \frac{\mathrm{Da}_6\theta_3}{|\mathcal{B}|}\left(|\Gamma^{(1)}| + |\Gamma^{(2)}|\right) + \mathrm{Pe}\epsilon\mathbf{u}_0 \cdot \nabla_{\boldsymbol{\xi}}\chi^{(3)[1]} - D^{(3)}\nabla^2_{\boldsymbol{\xi}}\chi^{(3)[1]} = 0 \quad \text{for } \boldsymbol{\xi} \in \mathcal{B}, \tag{C7a}$$

$$-\mathbf{n}^{(1)} \cdot D^{(3)}\nabla_{\boldsymbol{\xi}}\chi^{(3)[1]} = -\mathrm{Da}_5\theta_2 - \mathrm{Da}_6\theta_3 \quad \text{for } \boldsymbol{\xi} \in \Gamma^{(1)}, \tag{C7b}$$

$$-\mathbf{n}^{(2)} \cdot D^{(3)}\nabla_{\boldsymbol{\xi}}\chi^{(3)[1]} = -\mathrm{Da}_6\theta_3 \quad \text{for } \boldsymbol{\xi} \in \Gamma^{(2)}, \tag{C7c}$$

$$-\mathbf{n}^{(3)} \cdot D^{(3)}\nabla_{\boldsymbol{\xi}}\chi^{(3)[1]} = 0 \quad \text{for } \boldsymbol{\xi} \in \Gamma^{(3)}, \tag{C7d}$$

$$-\mathbf{n}^{(4)} \cdot D^{(3)}\nabla_{\boldsymbol{\xi}}\chi^{(3)[1]} = 0 \quad \text{for } \boldsymbol{\xi} \in \Gamma^{(4)}. \tag{C7e}$$

C32 Closure Problem for $\boldsymbol{\chi^{(3)[2]}}$

$$-\frac{\mathrm{Da}_6}{|\mathcal{B}|}\left(|\Gamma^{(1)}| + |\Gamma^{(2)}|\right) + \mathrm{Pe}\epsilon\mathbf{u}_0 \cdot \nabla_{\boldsymbol{\xi}}\chi^{(3)[2]} - D^{(3)}\nabla^2_{\boldsymbol{\xi}}\chi^{(3)[2]} = 0 \quad \text{for } \boldsymbol{\xi} \in \mathcal{B}, \tag{C8a}$$

$$-\mathbf{n}^{(1)} \cdot D^{(3)}\nabla_{\boldsymbol{\xi}}\chi^{(3)[2]} = \mathrm{Da}_6 \quad \text{for } \boldsymbol{\xi} \in \Gamma^{(1)}, \tag{C8b}$$

$$-\mathbf{n}^{(2)} \cdot D^{(3)}\nabla_{\boldsymbol{\xi}}\chi^{(3)[2]} = \mathrm{Da}_6 \quad \text{for } \boldsymbol{\xi} \in \Gamma^{(2)}, \tag{C8c}$$

$$-\mathbf{n}^{(3)} \cdot D^{(3)}\nabla_{\boldsymbol{\xi}}\chi^{(3)[2]} = 0 \quad \text{for } \boldsymbol{\xi} \in \Gamma^{(3)}, \tag{C8d}$$

$$-\mathbf{n}^{(4)} \cdot D^{(3)}\nabla_{\boldsymbol{\xi}}\chi^{(3)[2]} = 0 \quad \text{for } \boldsymbol{\xi} \in \Gamma^{(4)}. \tag{C8e}$$

C33 Closure Problem for $\boldsymbol{\chi^{(3)[3]}}$

$$-\frac{\mathrm{Da}_5}{|\mathcal{B}|}|\Gamma^{(1)}| + \mathrm{Pe}\epsilon\mathbf{u}_0 \cdot \nabla_{\boldsymbol{\xi}}\chi^{(3)[3]} - D^{(3)}\nabla^2_{\boldsymbol{\xi}}\chi^{(3)[3]} = 0 \quad \text{for } \boldsymbol{\xi} \in \mathcal{B}, \tag{C9a}$$

$$-\mathbf{n}^{(1)} \cdot D^{(3)}\nabla_{\boldsymbol{\xi}}\chi^{(3)[3]} = \mathrm{Da}_5 \quad \text{for } \boldsymbol{\xi} \in \Gamma^{(1)}, \tag{C9b}$$

$$-\mathbf{n}^{(2)} \cdot D^{(3)}\nabla_{\boldsymbol{\xi}}\chi^{(3)[3]} = 0 \quad \text{for } \boldsymbol{\xi} \in \Gamma^{(2)}, \tag{C9c}$$

$$-\mathbf{n}^{(3)} \cdot D^{(3)}\nabla_{\boldsymbol{\xi}}\chi^{(3)[3]} = 0 \quad \text{for } \boldsymbol{\xi} \in \Gamma^{(3)}, \tag{C9d}$$

$$-\mathbf{n}^{(4)} \cdot D^{(3)}\nabla_{\boldsymbol{\xi}}\chi^{(3)[3]} = 0 \quad \text{for } \boldsymbol{\xi} \in \Gamma^{(4)}. \tag{C9e}$$

C34 Closure Problem for $\boldsymbol{\chi^{(3)[4]}}$

$$\mathrm{Pe}\epsilon\left(\mathbf{u}_0 - \langle \mathbf{u}_0 \rangle_{\mathcal{B}}\right) + \mathrm{Pe}\epsilon \mathbf{u}_0 \cdot \nabla_{\boldsymbol{\xi}} \boldsymbol{\chi}^{(3)[4]} - D^{(3)} \nabla^2_{\boldsymbol{\xi}} \boldsymbol{\chi}^{(3)[4]} = \mathbf{0} \quad \text{for } \boldsymbol{\xi} \in \mathcal{B}, \tag{C10a}$$

$$-\mathbf{n}^{(1)} \cdot D^{(3)} \left(\mathbf{I} + \nabla_{\boldsymbol{\xi}} \boldsymbol{\chi}^{(3)[4]}\right) = \mathbf{0} \quad \text{for } \boldsymbol{\xi} \in \Gamma^{(1)}, \tag{C10b}$$

$$-\mathbf{n}^{(2)} \cdot D^{(3)} \left(\mathbf{I} + \nabla_{\boldsymbol{\xi}} \boldsymbol{\chi}^{(3)[4]}\right) = \mathbf{0} \quad \text{for } \boldsymbol{\xi} \in \Gamma^{(2)}, \tag{C10c}$$

$$-\mathbf{n}^{(3)} \cdot D^{(3)} \left(\mathbf{I} + \nabla_{\boldsymbol{\xi}} \boldsymbol{\chi}^{(3)[4]}\right) = \mathbf{0} \quad \text{for } \boldsymbol{\xi} \in \Gamma^{(3)}, \tag{C10d}$$

$$-\mathbf{n}^{(4)} \cdot D^{(3)} \left(\mathbf{I} + \nabla_{\boldsymbol{\xi}} \boldsymbol{\chi}^{(3)[4]}\right) = \mathbf{0} \quad \text{for } \boldsymbol{\xi} \in \Gamma^{(4)}. \tag{C10e}$$

C4 Closure Problems for $\boldsymbol{c_1^{(4)}}$:

C41 Closure Problem for $\boldsymbol{\chi^{(4)[1]}}$

$$\begin{aligned} &\frac{\mathrm{Da}_7 \theta_4}{|\mathcal{B}|}\left(|\Gamma^{(1)}| + |\Gamma^{(3)}| + |\Gamma^{(4)}|\right) + \frac{\mathrm{Da}_8 \theta_5}{|\mathcal{B}|}\left(|\Gamma^{(2)}| + |\Gamma^{(3)}| + |\Gamma^{(4)}|\right) \\ &\quad + \mathrm{Pe}\epsilon \mathbf{u}_0 \cdot \nabla_{\boldsymbol{\xi}} \chi^{(4)[1]} - D^{(4)} \nabla^2_{\boldsymbol{\xi}} \chi^{(4)[1]} = 0 \quad \text{for } \boldsymbol{\xi} \in \mathcal{B}, \end{aligned} \tag{C11a}$$

$$-\mathbf{n}^{(1)} \cdot D^{(4)} \nabla_{\boldsymbol{\xi}} \chi^{(4)[1]} = -\mathrm{Da}_7 \theta_4 \quad \text{for } \boldsymbol{\xi} \in \Gamma^{(1)}, \tag{C11b}$$

$$-\mathbf{n}^{(2)} \cdot D^{(4)} \nabla_{\boldsymbol{\xi}} \chi^{(4)[1]} = -\mathrm{Da}_8 \theta_5 \quad \text{for } \boldsymbol{\xi} \in \Gamma^{(2)}, \tag{C11c}$$

$$-\mathbf{n}^{(3)} \cdot D^{(4)} \nabla_{\boldsymbol{\xi}} \chi^{(4)[1]} = -\mathrm{Da}_7 \theta_4 - \mathrm{Da}_8 \theta_5 \quad \text{for } \boldsymbol{\xi} \in \Gamma^{(3)}, \tag{C11d}$$

$$-\mathbf{n}^{(4)} \cdot D^{(4)} \nabla_{\boldsymbol{\xi}} \chi^{(4)[1]} = -\mathrm{Da}_7 \theta_4 - \mathrm{Da}_8 \theta_5 \quad \text{for } \boldsymbol{\xi} \in \Gamma^{(4)}. \tag{C11e}$$

C42 Closure Problem for $\boldsymbol{\chi^{(4)[2]}}$

$$-\frac{\mathrm{Da}_7}{|\mathcal{B}|}\left(|\Gamma^{(1)}| + |\Gamma^{(3)}| + |\Gamma^{(4)}|\right) + \mathrm{Pe}\epsilon \mathbf{u}_0 \cdot \nabla_{\boldsymbol{\xi}} \chi^{(4)[2]} - D^{(4)} \nabla^2_{\boldsymbol{\xi}} \chi^{(4)[2]} = 0 \quad \text{for } \boldsymbol{\xi} \in \mathcal{B}, \tag{C12a}$$

$$-\mathbf{n}^{(1)} \cdot D^{(4)} \nabla_{\boldsymbol{\xi}} \chi^{(4)[2]} = \mathrm{Da}_7 \quad \text{for } \boldsymbol{\xi} \in \Gamma^{(1)}, \tag{C12b}$$

$$-\mathbf{n}^{(2)} \cdot D^{(4)} \nabla_{\boldsymbol{\xi}} \chi^{(4)[2]} = 0 \quad \text{for } \boldsymbol{\xi} \in \Gamma^{(2)}, \tag{C12c}$$

$$-\mathbf{n}^{(3)} \cdot D^{(4)} \nabla_{\boldsymbol{\xi}} \chi^{(4)[2]} = \mathrm{Da}_7 \quad \text{for } \boldsymbol{\xi} \in \Gamma^{(3)}, \tag{C12d}$$

$$-\mathbf{n}^{(4)} \cdot D^{(4)} \nabla_{\boldsymbol{\xi}} \chi^{(4)[2]} = \mathrm{Da}_7 \quad \text{for } \boldsymbol{\xi} \in \Gamma^{(4)}. \tag{C12e}$$

C43 Closure Problem for $\boldsymbol{\chi}^{(4)[3]}$

$$-\frac{\mathrm{Da}_8}{|\mathcal{B}|}\left(|\Gamma^{(2)}|+|\Gamma^{(3)}|+|\Gamma^{(4)}|\right)+\mathrm{Pe}\epsilon\mathbf{u}_0\cdot\nabla_{\boldsymbol{\xi}}\chi^{(4)[3]}-D^{(4)}\nabla^2_{\boldsymbol{\xi}}\chi^{(4)[3]}=0\quad\text{for }\boldsymbol{\xi}\in\mathcal{B},\tag{C13a}$$

$$-\mathbf{n}^{(1)}\cdot D^{(4)}\nabla_{\boldsymbol{\xi}}\chi^{(4)[3]}=0\quad\text{for }\boldsymbol{\xi}\in\Gamma^{(1)},\tag{C13b}$$

$$-\mathbf{n}^{(2)}\cdot D^{(4)}\nabla_{\boldsymbol{\xi}}\chi^{(4)[3]}=\mathrm{Da}_8\quad\text{for }\boldsymbol{\xi}\in\Gamma^{(2)},\tag{C13c}$$

$$-\mathbf{n}^{(3)}\cdot D^{(4)}\nabla_{\boldsymbol{\xi}}\chi^{(4)[3]}=\mathrm{Da}_8\quad\text{for }\boldsymbol{\xi}\in\Gamma^{(3)},\tag{C13d}$$

$$-\mathbf{n}^{(4)}\cdot D^{(4)}\nabla_{\boldsymbol{\xi}}\chi^{(4)[3]}=\mathrm{Da}_8\quad\text{for }\boldsymbol{\xi}\in\Gamma^{(4)}.\tag{C13e}$$

C44 Closure Problem for $\boldsymbol{\chi}^{(4)[4]}$

$$\mathrm{Pe}\epsilon\left(\mathbf{u}_0-\langle\mathbf{u}_0\rangle_{\mathcal{B}}\right)+\mathrm{Pe}\epsilon\mathbf{u}_0\cdot\nabla_{\boldsymbol{\xi}}\boldsymbol{\chi}^{(4)[4]}-D^{(4)}\nabla^2_{\boldsymbol{\xi}}\boldsymbol{\chi}^{(4)[4]}=\mathbf{0}\quad\text{for }\boldsymbol{\xi}\in\mathcal{B},\tag{C14a}$$

$$-\mathbf{n}^{(1)}\cdot D^{(4)}\left(\mathbf{I}+\nabla_{\boldsymbol{\xi}}\boldsymbol{\chi}^{(4)[4]}\right)=\mathbf{0}\quad\text{for }\boldsymbol{\xi}\in\Gamma^{(1)},\tag{C14b}$$

$$-\mathbf{n}^{(2)}\cdot D^{(4)}\left(\mathbf{I}+\nabla_{\boldsymbol{\xi}}\boldsymbol{\chi}^{(4)[4]}\right)=\mathbf{0}\quad\text{for }\boldsymbol{\xi}\in\Gamma^{(2)},\tag{C14c}$$

$$-\mathbf{n}^{(3)}\cdot D^{(4)}\left(\mathbf{I}+\nabla_{\boldsymbol{\xi}}\boldsymbol{\chi}^{(4)[4]}\right)=\mathbf{0}\quad\text{for }\boldsymbol{\xi}\in\Gamma^{(3)},\tag{C14d}$$

$$-\mathbf{n}^{(4)}\cdot D^{(4)}\left(\mathbf{I}+\nabla_{\boldsymbol{\xi}}\boldsymbol{\chi}^{(4)[4]}\right)=\mathbf{0}\quad\text{for }\boldsymbol{\xi}\in\Gamma^{(4)}.\tag{C14e}$$

Appendix D The Closure Solutions for the Nonlinear Homogeneous and Heterogeneous Reactions: Multiple Species

In this Appendix, we provide contour plots of the solutions to the closure problems recorded in Appendix C for the problem considering a multi-species system undergoing linear and nonlinear, homogeneous and heterogeneous reactions with multiple reactive interfaces. Due to $D^{(1)} = D^{(2)} = D^{(3)} = D^{(4)}$, we note that some closure variables have the same closure problems. For these variables, we solve the corresponding closure problem once and noted both variables in the contours.

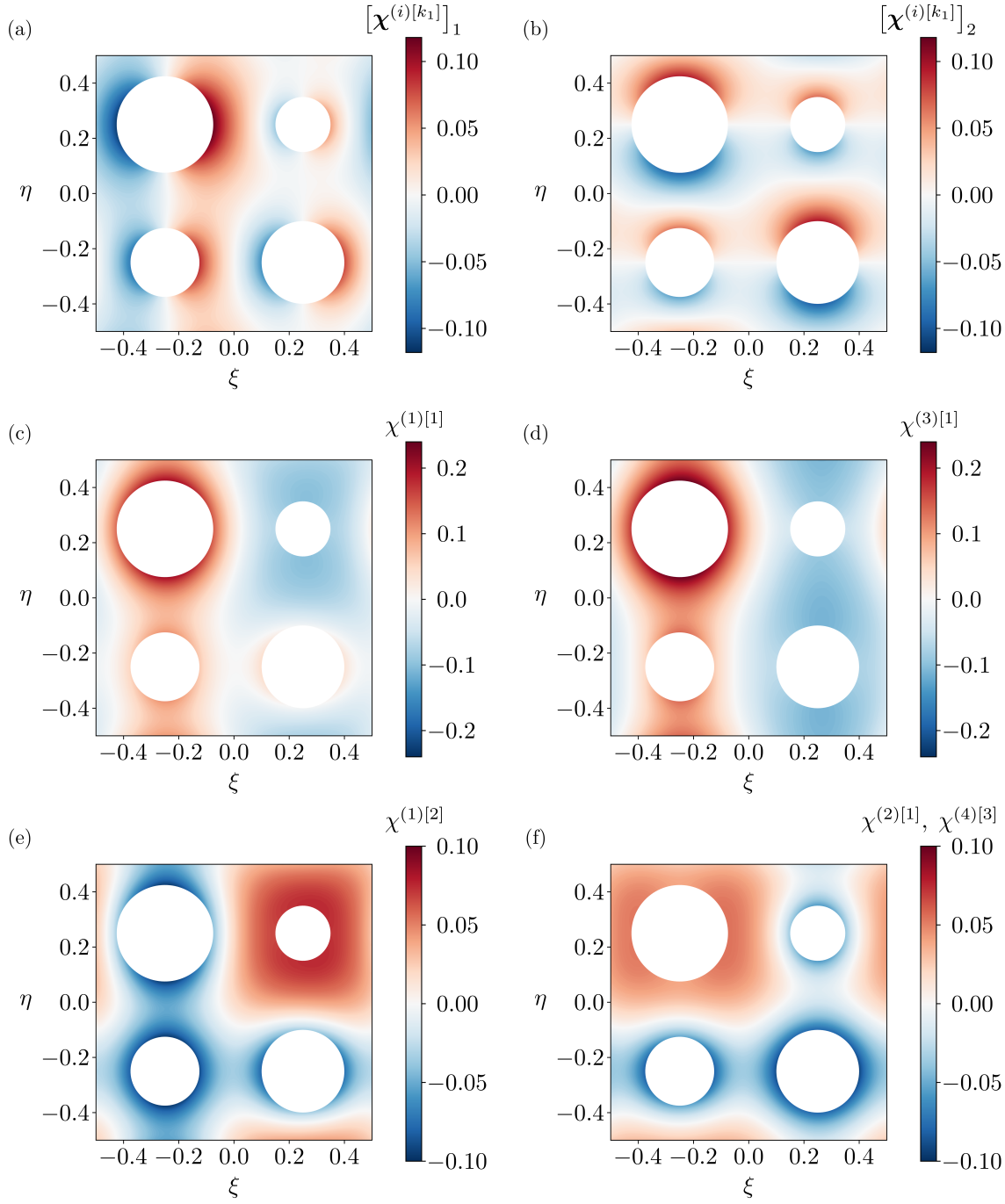

Figure D1. The numerical results of the closure problems in the unit-cell for the system involving multiple species undergoing linear and nonlinear, homogeneous and heterogeneous reactions. In (a) and (b), the contour plots of $[\boldsymbol{\chi}^{(i)[k_1]}]_1$, the resulting ξ-component of $\boldsymbol{\chi}^{(i)[k_1]}$, and $[\boldsymbol{\chi}^{(i)[k_1]}]_2$, the resulting η-component of $\boldsymbol{\chi}^{(i)[k_1]}$, are displayed respectively, where $k_1 \in \{4\}$ for $i \in \{1, 3, 4\}$, and $k_1 \in \{2\}$ for $i \in \{2\}$. (c) The contour plot of $\chi^{(1)[1]}$. (d) The contour plot of $\chi^{(3)[1]}$. (e) The contour plot of $\chi^{(1)[2]}$. (f) The contour plot of $\chi^{(2)[1]}$ and $\chi^{(4)[3]}$.

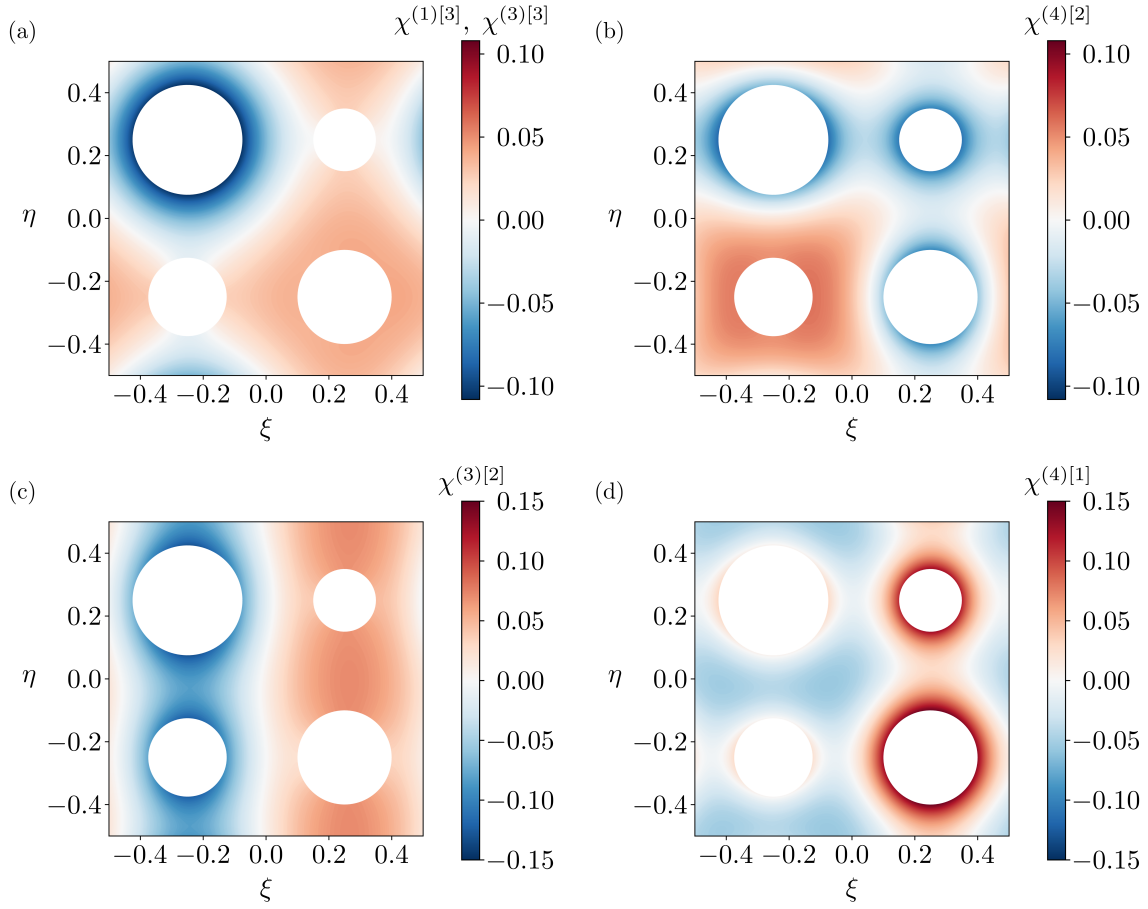

Figure D2. The numerical results of the closure problems in the unit-cell for the system involving multiple species undergoing linear and nonlinear, homogeneous and heterogeneous reactions. (a) The contour plot of $\chi^{(1)[3]}$ and $\chi^{(3)[3]}$. (b) The contour plot of $\chi^{(4)[2]}$. (c) The contour plot of $\chi^{(3)[2]}$. (d) The contour plot of $\chi^{(4)[1]}$.

References

Alnaes, M., Blechta, J., Hake, J., Johansson, A., Kehlet, B., Logg, A., ... Wells, G. (2015). The fenics project version 1.5. *Archive of Numerical Software*, *3*.

Auriault, J.-L., & Adler, P. (1995). Taylor dispersion in porous media: Analysis by multiple scale expansions. *Adv. Water Resour.*, *18*, 217-226.

Battiato, I., & Tartakovsky, D. (2011). Applicability regimes for macroscopic models of reactive transport in porous media. *J. Contam. Hydrol.*, *120-121*, 18-26.

Bloch, J.-F., & Auriault, J.-L. (2019). Upscaling of diffusion–reaction phenomena by homogenisation technique: Possible appearance of morphogenesis. *Transp. Porous Media*, *127*, 191-209.

Boso, F., & Battiato, I. (2013). Homogenizability conditions for multicomponent reactive transport. *Adv. Water Resour.*, *62*, 254-265.

Iliev, O., Mikelić, A., Prill, T., & Sherly, A. (2020). Homogenization approach to the upscaling of a reactive flow through particulate filters with wall integrated catalyst. *Adv. Water Resour.*, *146*. doi: 103779

Logg, A., Mardal, K.-A., & Wells, G. (2012). *Automated solution of differential equations by the finite element method*. Springer.

Pietrzyk, K., Korneev, S., Behandish, M., & Battiato, I. (2021). Upscaling and automation: Pushing the boundaries of multiscale modeling through symbolic computing. *Transp. Porous Media*, *140*, 313-349.

Figure 1.

1.) Identify the inhomogeneous terms of the system

$$\mathscr{F}[c_1] = -\mathbf{A}(\boldsymbol{\xi}) \cdot \mathbf{F}(t,\mathbf{x}) - \mathbf{B} \cdot \mathbf{F}(t,\mathbf{x}) + \frac{|\Gamma|}{|\mathcal{B}|} a(t,\mathbf{x}) + \nabla_{\boldsymbol{\xi}} \cdot \mathbf{F}(t,\mathbf{x}) \quad \text{in } \mathcal{B}$$

$$\mathscr{G}[c_1] = -\mathbf{n} \cdot \mathbf{F}(t,\mathbf{x}) + a(t,\mathbf{x}) \quad \text{on } \Gamma$$

2.) Use linearity to create a partial-solution and subsystem for each inhomogeneous term

$$c_1 = c_1^{\{1\}} + c_1^{\{2\}} + c_1^{\{3\}} + c_1^{\{4\}} + c_1^{\{5\}} + c_1^{\{6\}}$$

$$\mathscr{F}\left[c_1^{\{1\}}\right] = -\mathbf{A}(\boldsymbol{\xi}) \cdot \mathbf{F}(t,\mathbf{x}) \qquad \mathscr{G}\left[c_1^{\{1\}}\right] = 0$$

$$\mathscr{F}\left[c_1^{\{2\}}\right] = -\mathbf{B} \cdot \mathbf{F}(t,\mathbf{x}) \qquad \mathscr{G}\left[c_1^{\{2\}}\right] = 0$$

$$\mathscr{F}\left[c_1^{\{3\}}\right] = \frac{|\Gamma|}{|\mathcal{B}|} a(t,\mathbf{x}) \qquad \mathscr{G}\left[c_1^{\{3\}}\right] = 0$$

$$\vdots \qquad\qquad \vdots$$

3.) Consider valid closure forms for each partial-solution

$$c_1^{\{1\}} \in \left\{ \boldsymbol{\chi}_1^{\{1\}} \cdot \mathbf{F}(t,\mathbf{x}) + \overline{c}_1^{\{1\}} \right\}$$

$$c_1^{\{2\}} \in \left\{ \chi_1^{\{2\}} [\mathbf{B} \cdot \mathbf{F}(t,\mathbf{x})] + \overline{c}_1^{\{2\}}, \; \boldsymbol{\chi}_1^{\{2\}} \cdot \mathbf{F}(t,\mathbf{x}) + \overline{c}_1^{\{2\}} \right\}$$

$$c_1^{\{3\}} \in \left\{ \chi_1^{\{3\}} a(t,\mathbf{x}) + \overline{c}_1^{\{3\}} \right\}$$

$$\vdots$$

4.) Combine subsystems that emit partial-solutions of similar forms

Combine subsystems for $c_1^{\{1\}}$, $c_1^{\{2\}}$, $c_1^{\{4\}}$, $c_1^{\{5\}}$:

$$\mathscr{F}\left[c_1^{[1]}\right] = -\mathbf{A}(\boldsymbol{\xi}) \cdot \mathbf{F}(t,\mathbf{x}) - \mathbf{B} \cdot \mathbf{F}(t,\mathbf{x}) + \nabla_{\boldsymbol{\xi}} \cdot \mathbf{F}(t,\mathbf{x})$$

$$\mathscr{G}\left[c_1^{[1]}\right] = -\mathbf{n} \cdot \mathbf{F}(t,\mathbf{x})$$

$$c_1^{[1]} = \boldsymbol{\chi}_1^{[1]} \cdot \mathbf{F}(t,\mathbf{x}) + \overline{c}_1^{[1]}$$

Combine subsystems for $c_1^{\{3\}}$, $c_1^{\{6\}}$:

$$\mathscr{F}\left[c_1^{[2]}\right] = \frac{|\Gamma|}{|\mathcal{B}|} a(t,\mathbf{x})$$

$$\mathscr{G}\left[c_1^{[2]}\right] = a(t,\mathbf{x})$$

$$c_1^{[2]} = \chi_1^{[2]} a(t,\mathbf{x}) + \overline{c}_1^{[2]}$$

where $c_1 = c_1^{[1]} + c_1^{[2]}$

5.) Substitute partial-solutions into newly formed subsystems and simplify to obtain closure problems

Closure Problem 1:

$$\mathscr{F}\left[\boldsymbol{\chi}_1^{[1]}\right] = -\mathbf{A}(\boldsymbol{\xi}) - \mathbf{B} + \nabla_{\boldsymbol{\xi}} \cdot \mathbf{I} \quad \text{in } \mathcal{B}$$

$$\mathscr{G}\left[\boldsymbol{\chi}_1^{[1]}\right] = -\mathbf{n} \cdot \mathbf{I} \quad \text{on } \Gamma$$

Closure Problem 2:

$$\mathscr{F}\left[\chi_1^{[2]}\right] = \frac{|\Gamma|}{|\mathcal{B}|} \quad \text{in } \mathcal{B}$$

$$\mathscr{G}\left[\chi_1^{[2]}\right] = 1 \quad \text{on } \Gamma$$

Figure 2.

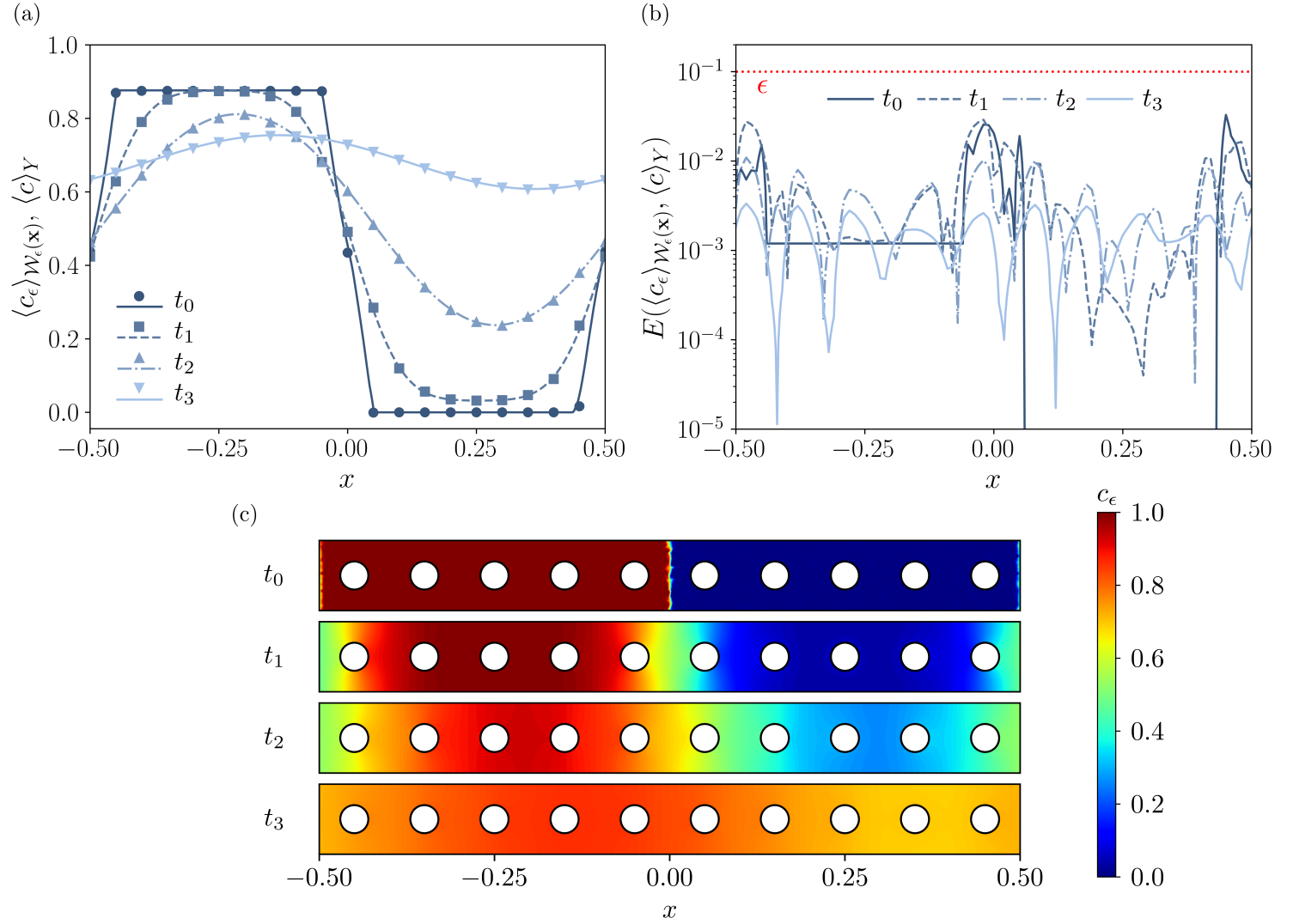
(a)
1.0
0.8
0.6
0.4
0.2
0.0
$\langle c_\epsilon \rangle_{\mathcal{W}_\epsilon(\mathbf{x})}$, $\langle c \rangle_Y$
t_0
t_1
t_2
t_3
−0.50
−0.25
0.00
0.25
0.50
x
(b)
10^{-1}
10^{-2}
10^{-3}
10^{-4}
10^{-5}
ϵ
t_0
t_1
t_2
t_3
$E(\langle c_\epsilon \rangle_{\mathcal{W}_\epsilon(\mathbf{x})}, \langle c \rangle_Y)$
−0.50
−0.25
0.00
0.25
0.50
x
(c)
t_0
t_1
t_2
t_3
−0.50
−0.25
0.00
0.25
0.50
x
c_ϵ
1.0
0.8
0.6
0.4
0.2
0.0

Figure 3.

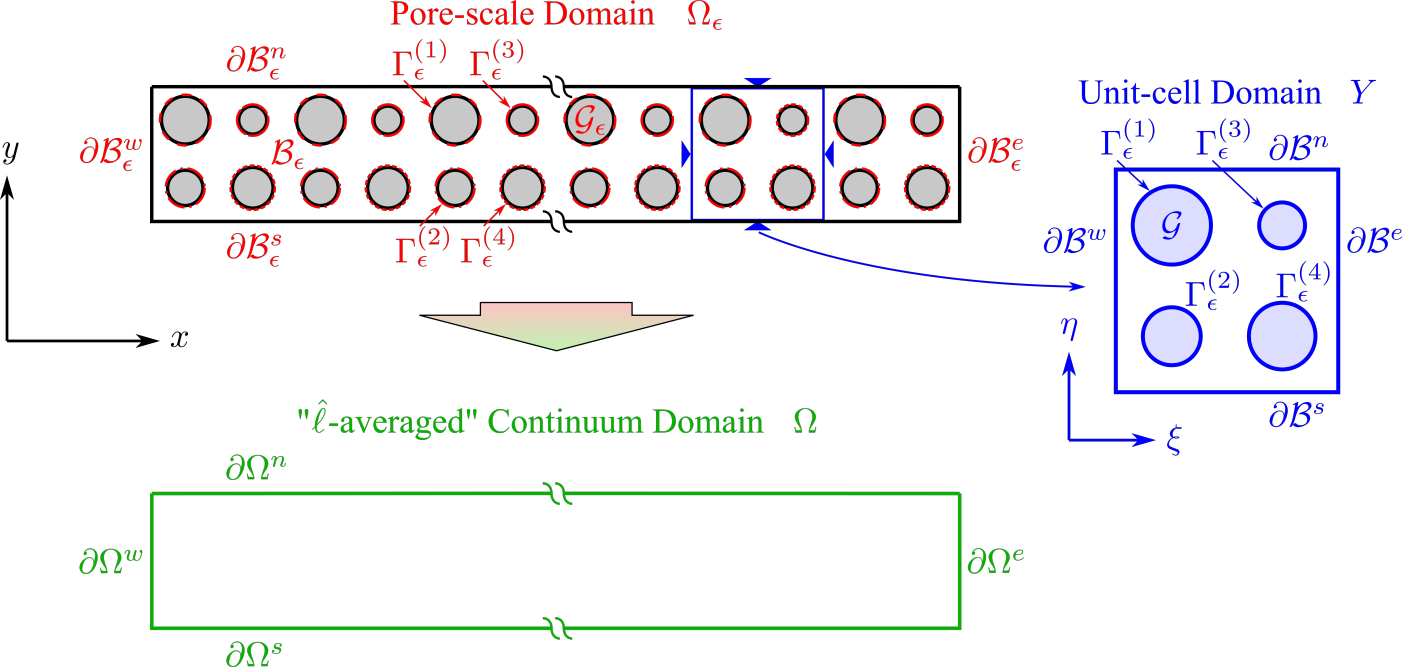
Pore-scale Domain Ω_ϵ
$\partial\mathcal{B}_\epsilon^n$
$\Gamma_\epsilon^{(1)}$
$\Gamma_\epsilon^{(3)}$
$\mathcal{G}_\epsilon$
$\partial\mathcal{B}_\epsilon^w$
$\mathcal{B}_\epsilon$
$\partial\mathcal{B}_\epsilon^e$
$\partial\mathcal{B}_\epsilon^s$
$\Gamma_\epsilon^{(2)}$
$\Gamma_\epsilon^{(4)}$
y
x
Unit-cell Domain Y
$\Gamma_\epsilon^{(1)}$
$\Gamma_\epsilon^{(3)}$
$\partial\mathcal{B}^n$
$\partial\mathcal{B}^w$
$\mathcal{G}$
$\partial\mathcal{B}^e$
$\Gamma_\epsilon^{(2)}$
$\Gamma_\epsilon^{(4)}$
η
ξ
$\partial\mathcal{B}^s$
"$\hat{\ell}$-averaged" Continuum Domain Ω
$\partial\Omega^n$
$\partial\Omega^w$
$\partial\Omega^e$
$\partial\Omega^s$

Figure 4.

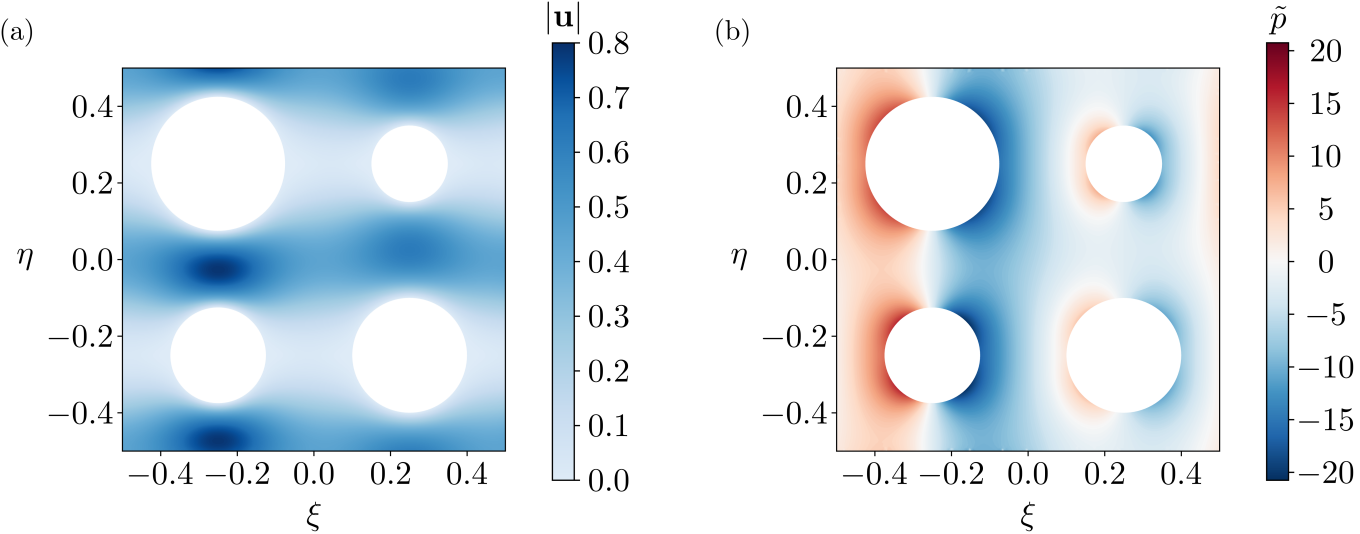
(a)
|u|
0.8
0.7
0.6
0.5
0.4
0.3
0.2
0.1
0.0
0.4
0.2
0.0
−0.2
−0.4
η
−0.4 −0.2 0.0 0.2 0.4
ξ
(b)
p̃
20
15
10
5
0
−5
−10
−15
−20
0.4
0.2
0.0
−0.2
−0.4
η
−0.4 −0.2 0.0 0.2 0.4
ξ

Figure 5.

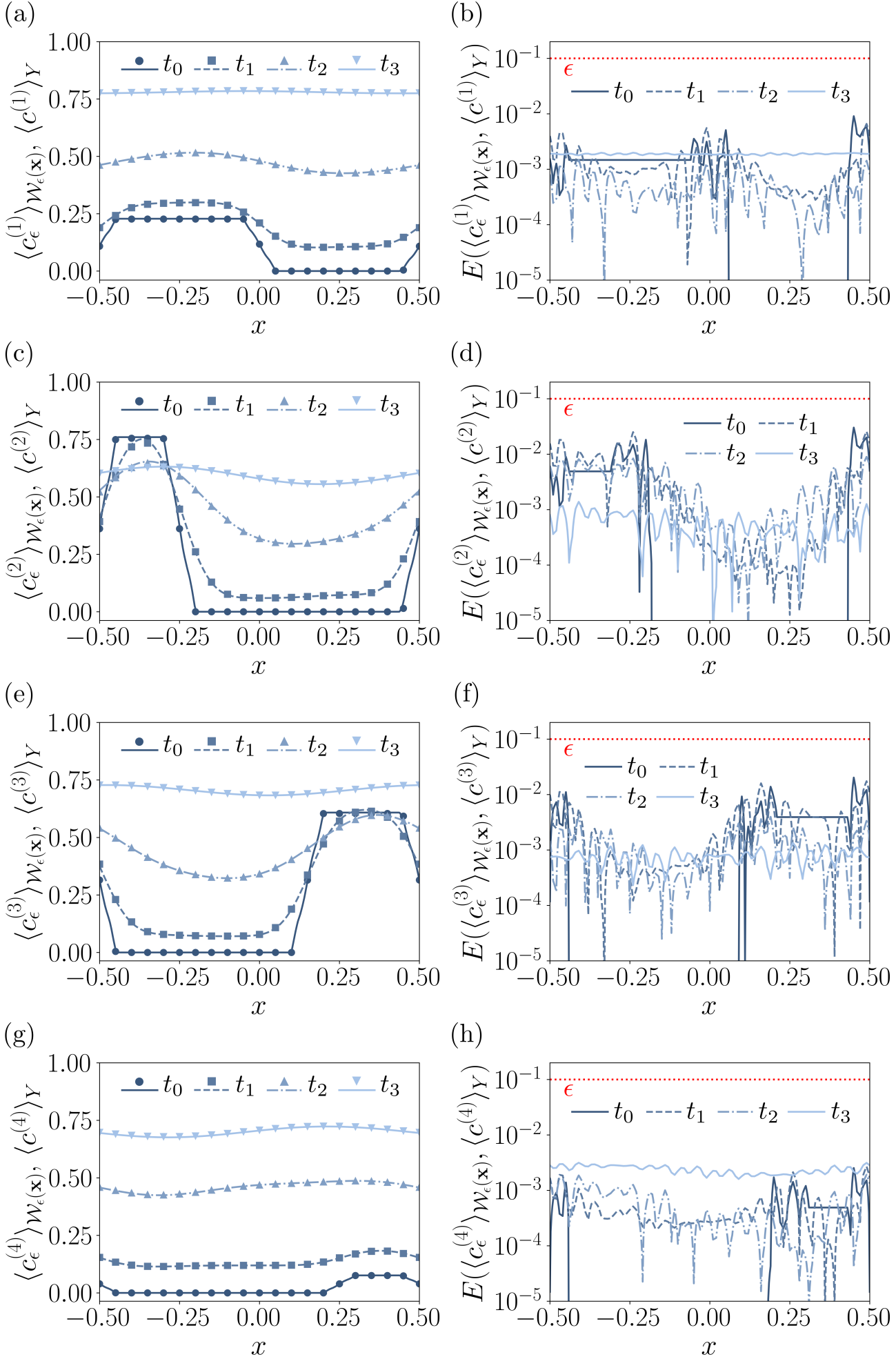
(a)
(b)
(c)
(d)
(e)
(f)
(g)
(h)
t_0 t_1 t_2 t_3
ϵ
x
$\langle c_\epsilon^{(1)} \rangle_{\mathcal{W}_\epsilon(\mathbf{x})}, \langle c^{(1)} \rangle_Y$
$E(\langle c_\epsilon^{(1)} \rangle_{\mathcal{W}_\epsilon(\mathbf{x})}, \langle c^{(1)} \rangle_Y)$
$\langle c_\epsilon^{(2)} \rangle_{\mathcal{W}_\epsilon(\mathbf{x})}, \langle c^{(2)} \rangle_Y$
$E(\langle c_\epsilon^{(2)} \rangle_{\mathcal{W}_\epsilon(\mathbf{x})}, \langle c^{(2)} \rangle_Y)$
$\langle c_\epsilon^{(3)} \rangle_{\mathcal{W}_\epsilon(\mathbf{x})}, \langle c^{(3)} \rangle_Y$
$E(\langle c_\epsilon^{(3)} \rangle_{\mathcal{W}_\epsilon(\mathbf{x})}, \langle c^{(3)} \rangle_Y)$
$\langle c_\epsilon^{(4)} \rangle_{\mathcal{W}_\epsilon(\mathbf{x})}, \langle c^{(4)} \rangle_Y$
$E(\langle c_\epsilon^{(4)} \rangle_{\mathcal{W}_\epsilon(\mathbf{x})}, \langle c^{(4)} \rangle_Y)$

Figure D1.

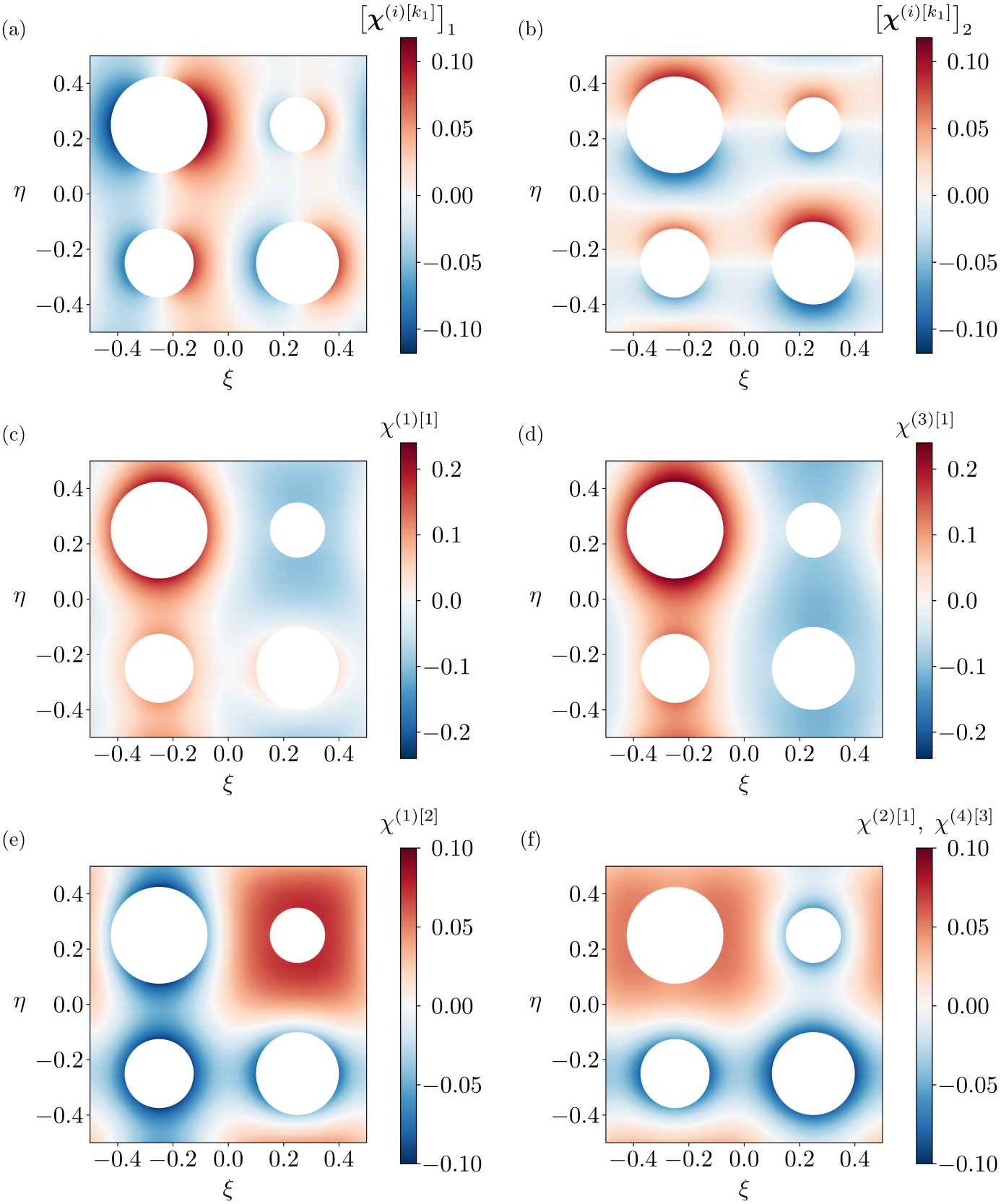
(a)
$[\chi^{(i)[k_1]}]_1$
(b)
$[\chi^{(i)[k_1]}]_2$
(c)
$\chi^{(1)[1]}$
(d)
$\chi^{(3)[1]}$
(e)
$\chi^{(1)[2]}$
(f)
$\chi^{(2)[1]}$, $\chi^{(4)[3]}$
ξ
η
0.4
0.2
0.0
−0.2
−0.4
0.10
0.05
0.00
−0.05
−0.10
0.2
0.1
0.0
−0.1
−0.2

Figure D2.

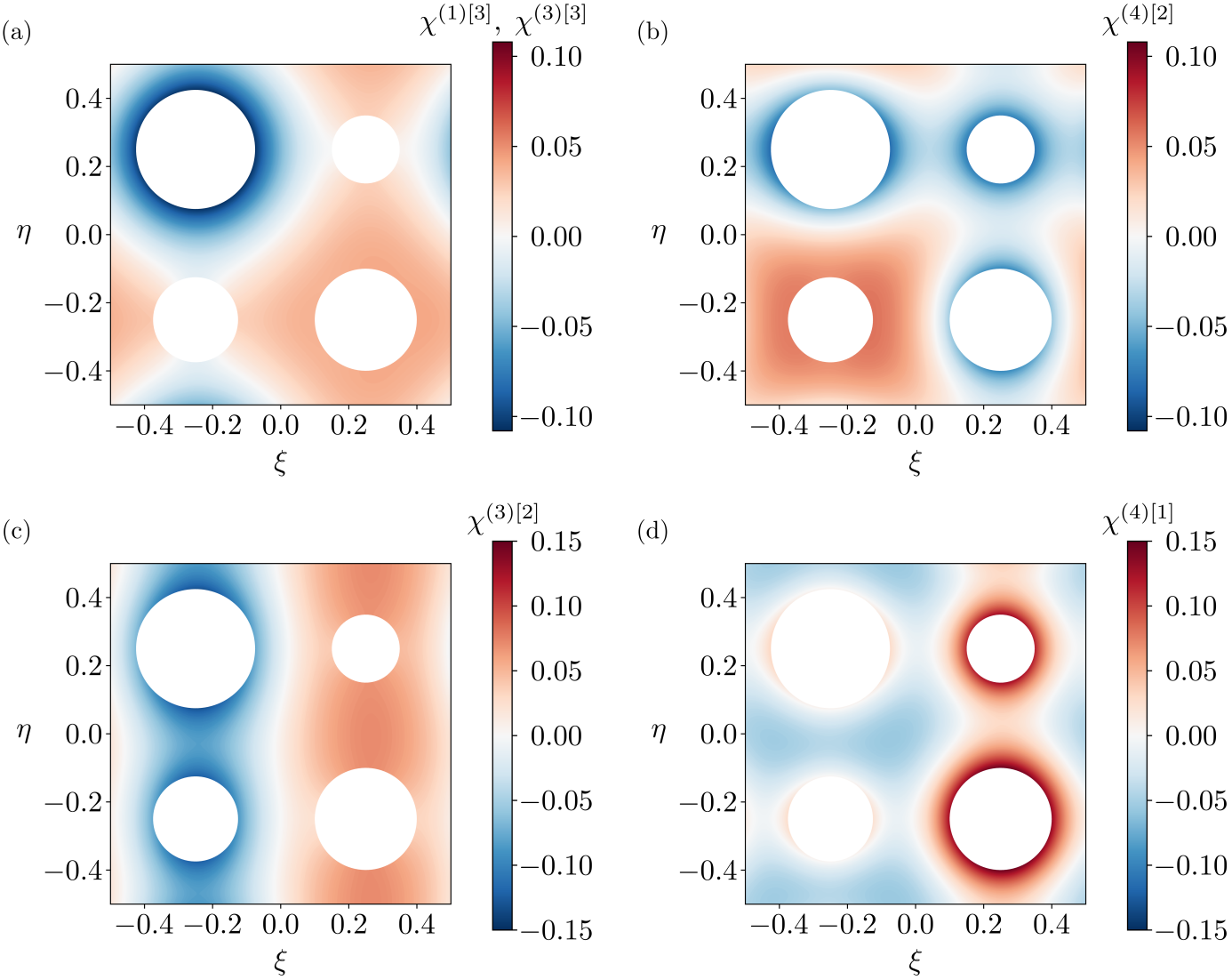
(a)
$\chi^{(1)[3]}$, $\chi^{(3)[3]}$
0.10
0.05
0.00
−0.05
−0.10
0.4
0.2
0.0
−0.2
−0.4
η
−0.4 −0.2 0.0 0.2 0.4
ξ
(b)
$\chi^{(4)[2]}$
0.10
0.05
0.00
−0.05
−0.10
0.4
0.2
0.0
−0.2
−0.4
η
−0.4 −0.2 0.0 0.2 0.4
ξ
(c)
$\chi^{(3)[2]}$
0.15
0.10
0.05
0.00
−0.05
−0.10
−0.15
0.4
0.2
0.0
−0.2
−0.4
η
−0.4 −0.2 0.0 0.2 0.4
ξ
(d)
$\chi^{(4)[1]}$
0.15
0.10
0.05
0.00
−0.05
−0.10
−0.15
0.4
0.2
0.0
−0.2
−0.4
η
−0.4 −0.2 0.0 0.2 0.4
ξ